

**Downscaling future climate projections to the watershed scale:
a North San Francisco Bay Estuary case study**

Elisabeth Micheli^a, Lorraine Flint^b, Alan Flint^b, Stuart Weiss^c, Morgan Kennedy^a

^a Dwight Center for Conservation Science at Pepperwood, Santa Rosa, CA 95404

^b U.S. Geological Survey, Sacramento CA 95819

^c Creekside Center for Earth Observation, Menlo Park CA 94025

ABSTRACT

We modeled the hydrology of basins draining into the northern portion of the San Francisco Bay Estuary (also known as North San Pablo Bay) using a regional water balance model (Basin Characterization Model; BCM) to estimate impacts of climate change at the watershed scale. The BCM calculates water balance components including runoff, recharge, evapotranspiration, soil moisture, and stream flow based on climate, topography, soils and underlying geology, and the solar-driven energy balance. We downscaled historical and projected precipitation and air temperature values derived from weather stations and global General Circulation Models (GCMs) to a spatial scale of 270 m. We then used the BCM to estimate hydrologic response to climate change for four scenarios spanning this century (2000-2100). Historical climate patterns show that Marin's coastal regions are typically on the order of 2 °C cooler and receive five percent more precipitation compared to the inland valleys of Sonoma and Napa due to marine influences and local topography. By the last 30 years of this century, the four scenarios analyzed here for the North Bay study area project average minimum temperatures to increase by 1.0 °C to 3.1 °C and average maximum temperatures to increase by 2.1 °C to 3.4 °C in comparison to conditions experienced over the last 30 years (1981-2010). Precipitation projections for the next century vary between GCMs (ranging from 2 to 15% wetter than the 20th century average). Across all scenarios, temperature forcing increases the variability of runoff, recharge, and stream discharge, and shifts hydrologic cycle timing. For both drier and wetter scenarios, warming amplifies climatic water deficit (a measure of drought stress on soils) by 8-21% by the close of the next century. Hydrologic variability within a single river basin demonstrated at the scale of subwatersheds may prove an important consideration for water managers in the face of climate change.

Key Words: climate change, watershed hydrology, downscaling, San Pablo Bay, Basin Characterization Model, stream flow, aquifer recharge, climatic water deficit.

Corresponding Author:

Lisa Micheli, lmicheli@pepperwoodpreserve.org, 707-591-9310 x 203

INTRODUCTION

Competently adapting to climate change requires watershed planning based on the best estimates science can provide of potential changes to local climate and the hydrologic cycle supporting our water resources other valuable ecosystem services. Application of projected climate data to evaluate impacts at the watershed scale requires downscaling from the 2.5 degree (approximately 250 km) spatial scale of current General Circulation Model (GCM) outputs. Downscaling entails the calculation of fine-scale information on the basis of coarser-scale information using various methods of statistical and spatial interpolation. New approaches to downscale GCM projections to finer spatial scales can reproduce empirically-validated results for air temperature and precipitation, providing the opportunity to apply physically-based models grounded in local watershed data to assess future climate impacts at meaningful hydrological and ecological scales (Flint and Flint 2011). The purpose of downscaling to the watershed scale is to create planning scenarios that adequately capture local climate variability. This variability may hold the key to helping managers identify zones of both watershed vulnerability and resilience in the face of climate change.

Applying these results effectively requires understanding limits to localized estimates of potential climate change. Watershed-scale climate and hydrology projections illustrate a range of planning scenarios capable of describing patterns and variability of historic climate data. Models can estimate ranges of natural variability, project directions and magnitude of decade to century trends, and quantify model uncertainty. Modeled scenarios are not intended to predict shorter term changes in weather, but instead project long-term climate trends based on a range of scenarios that provide realistic depictions of potential hydrology outcomes due to a warming climate. For effective adaptive management, real-time field data collection of watershed indicators will be crucial to testing hypotheses illustrated here via future climate scenarios.

SETTING

San Francisco's North Bay region (Figure 1) is a complex mosaic of land forms, vegetation types, land uses, and climate influences ranging from coastal to inland conditions (Weiss and others 2007). The jurisdiction of the North Bay Watershed Association (NBWA), the core of our study area, is comprised of approximately 2,200 km² comprising 25% of the watershed area draining directly into the San Francisco Bay Estuary. Nearly a half-million people live in the North Bay, less than 8% of the population of the entire Bay area (NBWA 2003). At the southern limit of California's North Coast Range, the region is tectonically active and typified by varied topography comprised of low mountain ranges framing north-south trending alluvial valleys. The majority of watersheds examined here drain directly to the San Francisco Bay (except for coastal Marin County, which drains directly to the Pacific Ocean and lies outside of NBWA's jurisdiction), and thus transition from rugged montane headwaters to depositional estuarine environments. Ecologically the Bay Area is considered a global "hotspot" of biodiversity, as biological diversity exploits the myriad of habitat types

generated by the climatic and geomorphic diversity of the region (Loarie and Ackerly 2004).

The major basins defined for this study form a west to east transect across the North Bay and include; “Marin Coast” (coastal drainages ranging from the Marin Headlands to Point Reyes), “Marin Bay” (Marin drainages discharging to the Bay), Petaluma River watershed, Sonoma Creek watershed, and the Napa River watershed (Figure 1). Excluding the Marin Coast basin, the core of the study area is comprised of the geographic jurisdiction of the NBWA. These major planning basins can be further divided into minor basins per watershed delineations generated by the Natural Resources Conservation Service’s California Interagency Watershed Mapping Committee (CalWater 1999, see Appendix A). Marin is the most densely populated area and is geologically distinguished by impermeable bedrock basins and limited aquifer recharge. Petaluma, Sonoma, and Napa support both urban and agricultural development including rural residential communities that dwell at the urban-wildland interface. North Bay communities rely on a varied portfolio of water sources—imported water (generally from sources further north) conveyed via aqueduct, surface storage, and where applicable, groundwater basins, where there is an emerging emphasis on conjunctive use of surface-groundwater supplies. Unlike the majority of California, snowmelt is not a significant component of the water cycle for the North Bay, although it may impact available imports.

Historic climate data for the North Bay reveals high spatial and temporal variability which adds to uncertainties associated with climate projections. In the context of global climate projections, the region is located in a transition zone between warmer and wetter winters projected for Oregon and Washington, and warmer and drier conditions projected for the south of California and Baja Mexico (Knowles and Cayan 2002; Cayan and others 2007, 2009). While average precipitation is therefore not consistently projected to shift towards a specifically wetter or drier climate, we selected GCM scenarios that project both more and ultimately less precipitation compared to historic conditions. Study results thus illustrate how projected increases in air temperatures for North Bay watersheds may impact the hydrologic cycle, particularly the relative ratios of evapotranspiration, runoff, and recharge, for both “wetter” and “drier” future scenarios.

METHODS

Basin Characterization Model

Watershed hydrology of North Bay drainages is the result of interactions between precipitation, surface water runoff, and infiltration (including direct recharge or groundwater interaction with streams, rivers and lakes). Runoff, recharge, and changes in soil moisture conditions can be estimated using a simple monthly water balance approach. The Basin Characterization Model (BCM) is a physically-based model that calculates water balance fractions based on data inputs for topography, soil composition

and depth, underlying bedrock geology, and spatially-distributed values (measured or estimated) of air temperature and precipitation (Flint and Flint 2007a, 2007b).

The BCM calculates monthly recharge and runoff using a deterministic water-balance approach based on the distribution of precipitation and the estimation of potential evapotranspiration (Flint and Flint 2007a, 2007b). The BCM relies on a rigorous hourly energy balance calculation using topographic shading and applies available spatial maps of elevation, bedrock permeability estimated from geology, soil water storage from STATSGO or SSURGO soil databases (NRCS 2006), vegetation density, and the empirically-based Parameter-Elevation Regressions on Independent Slopes Model (PRISM) precipitation and air temperature database and maps (Daly and others 2004). The BCM can be used to identify locations and climatic conditions that generate excess water by quantifying the amount of water available either as runoff or as in-place recharge on a monthly basis.

The BCM is calibrated regionally to measured potential evapotranspiration data and MODIS snow cover data (Flint and Flint 2007b, 2011). Locally, the model is also calibrated to measured unimpaired streamflow data. The determination of whether excess water becomes recharge or runoff is governed in part by the underlying bedrock permeability. The higher the bedrock permeability, the higher the recharge and the lower the runoff generated for a given grid cell. In small gaged basins that generate unimpaired flows, the bedrock permeability can be adjusted to calculate a total basin discharge that matches the measured basin discharge as shown in Figure 2. In the North Bay, eight stream gages shown in Figure 1 were used for model calibration. These gages are listed in Table 1 with their location description, USGS numerical identifier, and the ratio of measured data to modeled data for each period of record.

Temperature and precipitation are two primary drivers of physical processes acting at the watershed scale. BCM hydrologic variables sensitive to temperature include potential evapotranspiration (PET) and actual evapotranspiration (AET). BCM variables sensitive to quantities of precipitation include runoff and recharge. Climatic water deficit (CWD), defined in more detail below, combines the effects of precipitation inputs and temperature forcing by tracking soil moisture changes over time.

Characterizing Historic Patterns of Climate Variability

Historical values for monthly-averaged precipitation and air temperature are available in a gridded map format at a 4 km spatial scale from PRISM for the North Bay study area from 1896 through 2009 (Daly and others 2004). Spatial downscaling was performed on the coarse resolution grids (4 km) to produce fine resolution grids (270 m) using a model developed by Nalder and Wein (1998) modified with a “nugget effect” specified as the length of the coarse resolution grid (Flint and Flint 2011).

Our technique combines a spatial Gradient and Inverse Distance Squared (GIDS) weighting to monthly point data using multiple regressions calculated for every grid cell

for every month. Using the 4 km resolution digital elevation model in PRISM, parameter weighting is based on the location and elevation of the new fine resolution grid relative to existing coarse resolution grid cells (Flint and Flint 2011). To illustrate fine-scale geographic patterns of historic climate change over the last century, we applied a regression to the downscaled PRISM data for annual averages for every 270 m grid cell to calculate the magnitude and direction of observed changes in precipitation and air temperature for decade time intervals over the last century (Table 2).

Downscaling Future Climate Scenarios

Global future climate scenarios created through the application of General Circulation Models (GCMs) and distributed by the Intergovernmental Panel on Climate Change (IPCC) estimate future spatial patterns of temperature and precipitation in response to greenhouse gas forcing. GCMs are generally available for the continental US at 12 km spatial resolution (IPCC 2001, 2007). A set of these projections have been downscaled to 12 km for the State of California and its environs by researchers at USGS and Scripps Institute of Oceanography using the constructed analogs method of Hidalgo and others (2008), and provide a basis for our further downscaling for model application.

Our goal was to represent climate projections for California on the basis of global climate models that have proven capable of simulating recent historical climate, particularly the distribution of monthly temperatures and the strong seasonal cycle of precipitation that exists in the region (Knowles and Cayan 2002; Cayan and others 2007, 2009). In addition, models were selected to represent a range of model sensitivity to greenhouse gas forcing. On the basis of these criteria, two GCMs were selected, the Parallel Climate Model (PCM) developed by National Center for Atmospheric Research (NCAR) and Department of Energy (DOE) (see Washington and others 2000; Meehl and others 2003) and the National Oceanic and Atmospheric Administration (NOAA) Geophysical Fluid Dynamics Laboratory CM2.1 model (GFDL) (Stouffer and others 2006; Delworth and others 2006). The choice of greenhouse gas emissions scenarios included A2 (medium-high—essentially “business as usual”) and B1 (low—essentially a “mitigated emissions” scenario), was guided by considerations presented by the IPCC (Nakic’enoVIC and others 2000). Thus we developed a range of hydrology estimates based on four specific scenarios; two models each representing two emissions scenarios. We refer to these scenarios as “GFDL A2,” “GFDL B1,” “PCM A2,” “PCM A1.” For reasons described in detail below, we generalize GFDL scenarios as “warmer drier” and PCM scenarios as “warmer wetter.”

These four scenarios were downscaled from the 12 km grid scale to the historical PRISM data scale of 4 km for the purpose of bias correction. To make the correction possible the GCM is run for a historical forcing function to establish a baseline for modeling to match current climate. The baseline period for this study is defined as the PCM and GFDL model runs for 1950-2000 when climate change forcings are assumed absent from the model, representing current (pre-2000) atmospheric greenhouse gas conditions. This baseline period was then adjusted using the PRISM data from 1950-2000, for each

month and for each grid cell. Our approach to bias correction is a simple scaling of the mean and standard deviation of the projections to match those of the PRISM data following Bouwer and others (2004) and described in detail in Flint and Flint (2011). Once the bias correction is complete, the 4 km projections are further downscaled to 270 m spatial resolution using the GIDS spatial interpolation approach for model application.

Climatic Water Deficit

The term climatic water deficit defined by Stephenson (1998; Figure 3) is quantified as the amount of water by which potential evapotranspiration (PET) exceeds actual evapotranspiration (AET). This term effectively integrates the combined effects of solar radiation, evapotranspiration, and air temperature on watershed conditions given available soil moisture derived from precipitation. Climatic water deficit can be thought of as the amount of additional water that would have evaporated or transpired had it been present in the soils given the temperature forcing. This calculation is an estimate of drought stress on soils and plants and recent studies suggest it may serve as an effective control on vegetation cover types in the Bay Area (Cornwell 2010). In a Mediterranean climate, climatic water deficit can also be thought of as a surrogate for water demand based on irrigation needs, and changes in climatic water deficit effectively quantify the supplemental amount of water needed to maintain current vegetation cover, whether natural vegetation or agricultural crops.

BCM Data Analysis

The BCM estimates 16 hydrologic parameters at monthly time intervals for approximately two centuries over a set of grid points spaced 270 m apart. For the North Bay study area (approximately 2,820 km², NBWA jurisdiction plus Marin Coast major basin, Figure 1), this amounts to a data set comprised of approximately 38,680 monthly parameters spanning historic (1896-2000) and projected (2000-2100) time periods for four scenarios. Data was aggregated at the scales of CalWater minor basins, major planning basins, and the region as a whole (Appendix A). In analyzing and visually representing the data, average annual values were calculated for decades and 30-year time intervals to document long-term trends rather than displaying the details of variable inter-annual conditions. Maps of spatial distributions of parameters were made using sub-basins as the smallest unit of analysis, rather than displaying values at the scale of the 270 m grid (Figure 4A-F).

RESULTS

Historic Climate Variability

Analysis of historic PRISM data demonstrates that climate change in the North Bay is well underway yet patterns of change are highly variable spatially. Table 2 provides a summary of historical monthly values for key parameters averaged over decadal intervals. Average maximum temperatures have increased from 20.3 °C (1901-1910) to 21.7 °C (1991-2000), amounting to a net increase of 1.4 °C and an average rate of change of 0.014 °C y⁻¹. During this historical period there has also been a trend towards

increasing precipitation: for the first half of the century (1900 to 1950) annual precipitation averaged 752 mm y^{-1} versus an average of 845 mm y^{-1} (1951 to 2010) (12% greater) for the latter half of the century.

Mapped trends in precipitation and air temperature over the historical record for this area reveal the spatial variability underlying average regional values. Figure 4A shows the spatial distribution of average values for monthly precipitation, monthly maximum air temperature (T_{max}), and monthly minimum air temperature (T_{min}) for 1971-2000. High spatial variability is a product of coastal marine influences combined with variable topographic relief, which in turn creates topographic shading effects, cold air drainage, variation in adiabatic lapses in air temperature, and other controls on fine-scale climate.

Figure 4B displays the significant spatial variability in patterns of total change in climate over the same time period. Patterns of change show how localized areas of increases and decreases in precipitation and temperature are not uniform over the study area, variability which informs the interpretation of future projections. Trends in air temperature have been mostly warming, particularly over valley bottoms, while some zones of montane headwaters have experienced a cooling trend. The rate of change in minimum temperatures exceeds that for maximum temperatures, pointing to a recent trend in warmer nighttime and winter temperatures. The spatial distribution of change in climate is variable over the area with some locations changing more than others, suggesting that topographic features are influencing local climates in a manner to be taken into account in projecting future climates.

Regional Temperature and Precipitation Scenarios Derived from GCMs

By combining historic data derived from PRISM with projected temperature and precipitation values for four future scenarios we can compare model outputs with both the historic record and each other. Figure 5A-B displays comparable amounts of predicted warming for the GFDL and PCM models for both emissions scenarios but distinctly different precipitation signatures between GFDL and PCM models. The PCM model projects a significantly “wetter” future scenario than historic conditions or GFDL projections.

There is an insignificant separation between the GFDL and PCM models in average maximum temperatures projected by the century's close (2091-2100) for both the A2 ($25.1 \text{ }^{\circ}\text{C}$ and $24.8 \text{ }^{\circ}\text{C}$, respectively, with a resultant average of $25.0 \text{ }^{\circ}\text{C}$ for A2 scenarios) and the B1 ($23.9 \text{ }^{\circ}\text{C}$, both models) (Figure 5A). For the B1 scenarios this represents a rate of change of approximately $0.021 \text{ }^{\circ}\text{C y}^{-1}$ (1.5 times the 20th century rate of change) and for the A2 scenarios this results in a rate of change of approximately $0.032 \text{ }^{\circ}\text{C y}^{-1}$ (2.3 times the 20th century rate of change). While there is some variation in slope, the total change over time is relatively steady. This series demonstrates a close alignment between the GFDL A2 and PCM A2 scenarios and between the GFDL B1 and PCM B1 scenarios in terms of temperature projections despite variations between decades.

Figure 5B shows that projected precipitation is highly variable in terms of projected long-term trends. In contrast to temperature projections, model algorithm (GFDL versus PCM) is more important than emissions scenarios in driving projected precipitation. Compared to the 20th century average of $799 \pm 280 \text{ mm y}^{-1}$ (1901-2000), the average precipitation for the two GFDL scenarios (2001-2100) is 819 mm y^{-1} (2% greater than 20th century) while the average precipitation for the two PCM scenarios (2001-2100) is 918 mm y^{-1} (15% greater than 20th century). While century-scale averages remain in the range of historic variability, values projected for individual decades display unprecedented wet and dry periods. The B1 scenarios for both models project unprecedented peaks in the first half of the century (GFDL B1 projects $1,088 \pm 179 \text{ mm y}^{-1}$ for 2011-2020, PCM B1 projects $1,192 \pm 181 \text{ mm y}^{-1}$ for 2021-2030). By the next century's close, the GFDL and PCM models diverge, with the greatest contrast in 2081-2090 when the GFDL A2 projects an unprecedented drought averaging only $569 \pm 80 \text{ mm y}^{-1}$ while for the same period the PCM A2 projects $1,067 \pm 188 \text{ mm y}^{-1}$.

By the century's close, the four scenarios may be distinguished by emissions scenarios defining two different temperature futures (A2 and B1, as listed above) and a range of potential precipitation projections depending on whether the GFDL or the PCM model is applied. By the 2091-2100 time interval, the wetter-warmer PCM model for the A2 and B1 scenarios is characterized by an average precipitation value of $910 \pm 115 \text{ mm y}^{-1}$ (14% more than the 20th century average) versus a warmer-drier GFDL model average for the A2 and B1 scenarios of $725 \pm 79 \text{ mm y}^{-1}$ (9% less than the 20th century average). This is the basis for terming GFDL projections "warmer drier" versus PCM projections as "warmer wetter" in proceeding sections.

Basin Characterization Model Results: Future Hydrology Scenarios

Figure 6A-N displays time series data (with average values based on monthly values) for the GFDL A2 and PCM A2 scenarios for the last and current centuries in 30-year intervals (the exception is the 1896-1910 interval which represents only 25 years). Plots thus combine historic data for the last century with projected data for the next starting in 1896 and closing in 2100. These results are summarized in Table 3, which also displays values for B1 emissions scenarios not shown in Figure 6A-N. Values displayed from 1896 to 2000 are derived from PRISM, while values from 2000 to 2100 are a combination of GCM outputs for temperature and precipitation (summarized above) and modeled BCM outputs for hydrologic variables. The left sides of Figure 6A-N display annual data distributions for 30 year intervals including box plots scaled vertically to the standard deviation and with "whiskers" scaled to the 5 to 95% confidence interval. The right side of the data plots show the frequency distribution of annual values compiled for each 30-year time interval.

Trends in runoff and recharge

Under both projected scenarios (GFDL A2 and PCM A2) histograms of annual precipitation values shown in Figure 6E-F show a wide distribution relative to historic conditions, with unprecedented annual extremes (represented by maxima in excess of

2,000 mm y^{-1}) and a concentration of the remainder of events in the lower range of the historic record. This indicates a shift away from the historic distribution where the centroid of the distribution is concentrated around the mean of record, with a dominance of relatively moderate annual average precipitation values (approximately 800 ± 250 mm y^{-1}). The response of hydrologic variables including runoff and recharge is highly sensitive to variation in precipitation over time and between scenarios. The diversity of estimated precipitation regimes across the suite of four scenarios shown in Figure 7 implies that a broad range of possible combinations of temperature and precipitation are modeled in the course of this study. The trend of spreading the width of distributions towards formerly rare or even unprecedented precipitation extremes drives variability in runoff and recharge for all scenarios.

Distributions of average annual values for runoff (Figure 6G-H) for both scenarios mirror the increasing spread of precipitation values, indicating more extreme events at both ends of a range that includes unprecedented extreme wet values for average annual runoff compared to a 20th century average of 227 ± 154 mm y^{-1} (1901-2000). For the GFDL A2 scenario, by this century's close (2071-2100) estimated annual average runoff is 187 ± 27 mm y^{-1} (18% lower than the 20th century average). For the PCM A2 scenario, by this century's close (2071 to 2100) average annual runoff is estimated at 313 ± 50 mm y^{-1} (38% higher than the 20th century average).

For recharge, Figure 6I-J shows that both models project increases in the first half of the next century in response to increased precipitation. However, the full distribution of average annual values trends towards more frequent occurrences of low recharge years with infrequent high recharge years. Paralleling runoff, this distribution includes more extreme annual events compared to the more consistent pattern of annual values concentrated around the mean of record observed in historic time steps. For the GFDL A2 scenario, by this century's close (2071 to 2100) estimated average annual recharge is 89 ± 10 mm y^{-1} (6% lower than the 20th century average). For the PCM A2 scenario, by this century's close (2071 to 2100) average estimated recharge is 131 ± 17 mm y^{-1} (39% higher than the 20th century average).

Trends in evapotranspiration

Figure 6A-B shows an increasing trend in temperature of approximately $0.03^{\circ}\text{C } y^{-1}$ (between the 1981-2010 and 2071-2100 time intervals), which in turn drives increases in estimated potential evapotranspiration (PET) shown in Figure 6K-L. While the 20th century rate of change for PET was approximately 0.22 mm y^{-1} , the A2 scenarios project PET to increase at a rate of approximately 0.56 to 0.74 mm y^{-1} . The net effect of the accelerated rate of change in PET due to temperature forcing is that by next century's close (2071 to 2100), average PET is projected to range from $1,268$ mm y^{-1} (PCM A2) to $1,286$ mm y^{-1} (GFDL A2). The entire span of annual values projected for 2071 to 2100 exceed the distribution of annual values for the first historic time interval (1896 to 1920). This amounts to an increase on the order of 7-8% (compared to the 20th century

average) in average annual PET (approximately 100 mm of water or 13% of 20th century average annual precipitation) for both drier and wetter scenarios.

Trends in climatic water deficit

Climatic water deficit (CWD) is projected to increase over this century a rate ranging from 0.25 to 1.5 mm y⁻¹ depending on whether a wetter or drier scenario is used (PCM B1 and GFDL A2, respectively). For the PCM A2 scenario, by this century's close (2071 to 2100) average estimated CWD is 758 ± 20 mm y⁻¹ (8% higher than the 20th century average). For the GFDL A2 scenario, by this century's close (2071 to 2100) average estimated CWD is 855 ± 19 mm y⁻¹ (21% higher than the 20th century average). Thus while the wetter scenario projects a 15% increase in precipitation and runoff compared to historical (20th century) conditions, this additional water does not offset drought stress to soils, and as a result there is still a soil drying trend on the order of 50% the effect estimated for the lower precipitation scenario.

Trends in water balance partitioning

Figure 8 shows partitioning of the water balance over time. Visually subtle variations shown here have significant impacts in terms of determining whether watersheds experience drought versus adequate water supply, underscoring that small tradeoffs (5-10%) between water balance terms can have big impacts in terms of watershed condition. For an average decade shown here, the sum of plotted terms is 797 mm (equivalent to precipitation plus change in soil storage, with soil storage typically on the order of 1-3% of the water balance), with approximately 59% in actual evapotranspiration (AET), 12% in recharge, and 28% in runoff. Note that for the wettest decade shown here, the sum of plotted terms is 940 mm, with approximately 57% in AET, 14% in recharge, and 29% in runoff, which are relatively close to the average values. By contrast, for the driest decade on record, the sum of the plotted terms is 575 mm, with approximately 69% in AET, 10% in recharge, and 21% in runoff. Thus as conditions trend toward those typified by the driest decade predicted here, a larger fraction of the total water available is "lost" to evapotranspiration, leaving approximately 10% less water (on the order of 60-90 mm water per year) available for recharge and runoff.

Projected Spatial Distribution of Runoff, Recharge, and Climatic Water Deficit

The sequence of maps shown in Figure 9A-F depicts the percentage change in runoff, recharge, and climatic water deficit calculated between the average of 1971-2000 and the average of 2071-2100 for the GFDL and PCM models for the A2 scenario. Represented average values are plotted at the scale of minor basins. The resilience of individual minor basins to future changes in climate is a function of interactions between topography, solar orientation, soils, and geology. These maps illustrate the relative vulnerability and resilience of the various minor basins to future changes in climate by the relative changes over the 100-yr period. The most notable difference among the maps is between models, with the PCM model projecting less drought stress than the GFDL model. Spatial trends reflect the moderating effect of coastal marine

climates, with lower changes in the future for all variables, especially the climatic water deficit, for basins located nearer to the coast. Minor basins characterized by thick alluvium over valley bottoms provide both the opportunity for greatest recharge and risk of greatest climatic water deficit. An understanding of the variability between minor basins can help to characterize hydrologic response at a scale useful for management.

Projected Climate Change Impacts on Stream Flow and Basin Recharge

Stream flow and estimated basin recharge integrates many responses of the basin to variation in climate. Evaluating patterns of basin discharge or stream flow over time at the scale of a three-year running average helps to discern potential future frequencies of both wet periods and drought. These analyses can be conducted at the scales of the region as a whole, for a river (major) basin at a gauged location, or for a minor basin (sub-watershed). In this section we demonstrate analyses that can be conducted using study results at all three scales.

BCM simulations enable viewing stream discharge data as a time series. We chose to display discharge as a three-year running average to be consistent with what water agencies typically use to evaluate potential drought conditions (with a drought typically considered to be comprised of three contiguous dry years). Figure 10A displays impacts on runoff available for stream flow at the scale of the entire region and Figure 10B represents historic and projected stream flow for the Napa River at the Saint Helena gage in terms of three-year running averages.

Figure 10A shows that for the region as a whole, annual amounts of runoff available as stream discharge averaged $452 \times 10^6 \text{ m}^3$ during the 20th century. For this century, the GFDL A2 scenario estimates an average of $445 \times 10^6 \text{ m}^3$ runoff available for streamflow (2% less than the 20th century average), while the PCM A2 estimates $539 \times 10^6 \text{ m}^3$ runoff available for streamflow (19% more than the 20th century average) based on mean three-year running average values.

Figure 10B shows that for the Napa River at Saint Helena the historic record (1940-2007) displayed a mean three-year running average value of $10.4 \times 10^6 \text{ m}^3$. The GFDL A2 scenario averaged $10.1 \times 10^6 \text{ m}^3$ while PCM A2 scenario averaged $13.7 \times 10^6 \text{ m}^3$. The PCM A2 series includes 8 three-year average values that exceed the maximum three-year average value of the historic record ($19.2 \times 10^6 \text{ m}^3$). The GFDL A2 series includes 3 three-year average values that exceed the maximum three-year average of the historic record, and one three-year average value that is less than the minimum three-year average of the historic record ($3.4 \times 10^6 \text{ m}^3$). In terms of underlying annual values for stream discharge, the GFDL A2 scenario displays that for 15 out of 90 years flows would be below the previous annual minimum of record.

River managers and engineers typically rely on frequency plots of cumulative discharge for sizing hydraulic structures and stream channel restorations. Figure 11 shows the

cumulative probability of annual stream discharge for the Napa River at Saint Helena with a historic frequency curve (1971-2000) compared to estimated values under the GFDL A2 and PCM A2 scenarios (2071-2100). This plot shows that future scenarios project shifts in the negative direction under GFDL A2 and shifts in the positive direction for PCM A2. For example, if one examines values estimated for a return frequency of 0.5, which estimates the average discharge of the system, the historic value is $93.7 \times 10^6 \text{ m}^3$ versus a projected value of $65.3 \times 10^6 \text{ m}^3$ for the GFDL A2 scenario and a projected value of $110.2 \times 10^6 \text{ m}^3$ for the PCM A2 scenario.

Frequency plots can also be created using three-year average discharge and recharge values to show managers potential shifts in discharge frequencies for minor planning basins. Figure 12 shows vertical histograms that compare runoff available for stream discharge and estimated basin recharge for the minor basin of the Napa River known as Milliken Creek. This plot shows that while in 1971 to 2000, available runoff exceeded $1000 \times 10^3 \text{ m}^3$ 57% of the time. Under the GFDL A2 scenario for 2071-2100, this threshold would be exceeded only 23% of the time. In terms of basin recharge, while for the historic period (1971-2000) basin recharge exceeded $500 \times 10^3 \text{ m}^3$ 74% of the time, under the GFDL A2 scenario for 2071-2100, this threshold would be exceeded only 36% of the time.

Projected Climate Change Impacts on Timing of Water Availability

The BCM generates monthly estimates for all hydrologic parameters, which facilitates an examination of the potential impacts of climate change on hydrologic seasonality. Figure 13A-D compares average values by month for precipitation, runoff, recharge, and potential evapotranspiration for recent conditions (1981-2010) and projected conditions under GFDL A2 and PCM A2 (2071-2100). Both projected scenarios display significant reductions in early wet season rainfall, and while PCM A2 projects significantly higher rainfall in January, February and March, it joins the GFDL A2 scenario in projecting drier conditions in April, May and June than for the recent time period (Figure 13A). This pattern is reiterated in seasonal patterns of runoff and recharge (Figure 13B-C). Figure 13D shows that both future scenarios show increased potential evapotranspiration during the months of May through September, which is likely to increase water demand regardless of variations in rainfall during antecedent winter months.

Comparative Analysis of Major North Bay Basins

Figure 14A-N plots values calculated for the five major basins of the North Bay for all variables analyzed using the BCM for the historic (1896-2009) and projected (2010-2100) time periods. These plots show an approximate 0.5 to 1.0 °C separation between each major basin and the set of Sonoma and Napa (which are highly similar), in terms of maximum temperatures (Figure 14A-B). For minimum temperatures, Marin Bay emerges as consistently on the order of 1.0 °C warmer than the remainder of basins characterized by more significant inland valleys, a set which shows less than 0.25 °C separation among each other during the historical period, and displays a trend towards becoming even more convergent by the century's close (Figure 14C-D). Plots for

precipitation (Figure 14E-F) display the spatial variability between basins and significant differences between the PCM and GFDL model in terms of estimated rainfall by the century's close: for 2071-2100 time period, the GFDL A2 scenario precipitation estimates range from 619 mm y^{-1} for the Petaluma River basin to 790 mm y^{-1} for the Marin Coast, while under the PCM A2 scenario ranges from 836 mm y^{-1} for the Petaluma River basin to 1,023 mm y^{-1} for the Marin Coast.

Plots of estimated runoff (Figure 14G-H) and recharge (Figure 14I-J) reflect varying amounts of projected precipitation between scenarios and over time, but also show the impact of specific major basin characteristics. Particularly given climate change projections, the capacity of deep alluvium deposits in basins with significant valley formations provide the opportunity for significant recharge gains (at the expense of runoff), especially in Napa and Sonoma, under high precipitation scenarios (Figure 14J). Lacking subsurface storage capacity, the Marin Coast and Bay basins show a tendency towards converting increased precipitation directly to runoff (Figure 14 I-J).

Under both scenarios, regardless of variations in precipitation, potential evapotranspiration and climatic water deficit are projected to steadily climb through time for all basins (Figure 14K-N). Climatic water deficit shows a steeper rate of change than potential evapotranspiration for the GFDL A2 scenario (Figure 14M). Higher quantities of excess rainfall mitigate this effect for the PCM A2 scenario (Figure 14N). Napa and Sonoma, with the largest areas of inland valleys prone to warming, display on the order of 50 mm y^{-1} greater climatic water deficit than the Marin Coast (Figure 14M-N).

Conclusions

- The North Bay has already experienced a significant warming trend over the last century with monthly maximum temperatures having increased approximately 1.4 °C between 1901 and 2000.
- The spatial distribution of climate change to date is variable, with a trend towards warming of valley bottoms and in some cases cooling of montane areas. Coastal influences in general mitigate the warming trend, such that affects are more pronounced with increasing distance from the Pacific Coast or the Bay.
- There is more uncertainty in projected precipitation trends than in projected temperature trends. The two climate models analyzed in this study represent the implications of future precipitation remaining comparable to today's versus a wetter future (approximately 20% more precipitation) in the context of a warmer climate.
- Historic patterns of precipitation are highly variable, and given the effects of temperature forcing on coupled climate-hydrologic processes, temporal and

spatial variability of precipitation, runoff, recharge, and stream discharge is likely to increase.

- Hydrologic models predict reduced early and late wet season runoff for the next century, resulting in a potentially extended dry season, for both wetter and drier future climate scenarios. Scenarios that estimate increased precipitation project that precipitation to be concentrated in midwinter months, a trend which could increase risk of floods.
- Evapotranspiration and associated climatic water deficit is projected to steadily increase in both the wetter and drier future scenarios, with values for the 2071-2100 period projected to be 5 to 20 % higher than the 1981-2010 period, which translates to approximately 40 to 150 mm additional water needed on average to maintain current soil moisture conditions. Summers are projected to be longer and drier in the future than in the past regardless of precipitation trends.
- While water supply may be subject to increased variability (e.g. reduced reliability) due to higher variability in precipitation, water demand is likely to steadily increase due to increased rates of evapotranspiration and climatic water deficit during extended summers.
- Extended dry season conditions and the potential for extended drought combined with unprecedented precipitation events may serve as additional stressors on water quality and habitat.
- Real-time monitoring of hydrological variables, as laid out in the NBWA *Watershed Indicators* report (Ridolfi and others 2010) and related efforts, will be central to testing hypotheses about potential climate change demonstrated in this report and equipping managers to respond to climate adaptation challenges in a timely fashion.

Discussion: Applications to Management

For adaptive resource management, it is central to develop scenarios using models capable of accurately representing historical regional climate and hydrology. Physically-based watershed models and finely downscaled climate projections can effectively represent environmental processes at local scales and can be used to generate planning scenarios that incorporate climate impacts on the water cycle. Assessing impacts to the hydrologic cycle will be central to effective water resource planning. These models benefit from using empirical topography, soils, and geologic data at the finest spatial and temporal resolution available. Managers should not rely on these projections for specific short term weather predictions, but rather for identification of potential long-term underlying trends operating at the decadal to century scales.

While general circulation models (GCMs) converge on consistent temperature projections for the region given a range of emissions scenarios, they do not provide consistent projections regarding future precipitation. The discrepancy between the models is due to assumptions regarding long-term climate cycles over the Pacific Ocean and the relative arbitrariness of assigning a particular time value to start or end such a cycle in the process of modeling. Thus it is important for watershed managers to consider a range of future precipitation scenarios and impacts on runoff, recharge, and climatic water deficit. Arguably, the higher the projected rate of climate change for a sub-basin, the more vulnerable resources may be in terms of the adaptation challenge.

It is worth noting, according to Cayan and others (2008), that a 10–20% change in annual precipitation is not a minor gain or loss. In the historical record, a 15% loss in precipitation is sufficient to cast a year into the lowest third of the annual totals, and, since runoff is a non-linear outcome of precipitation, lessening the supply can in many cases drive runoff disproportionately lower.

Recharge is less sensitive to variability in precipitation than runoff. The impact of variable precipitation on rates of recharge appear dampened during dry periods and exaggerated during wet periods, an effect that can be demonstrated using average values for the 2071-2100 time interval relative to historic means. In the drier GFDL A2 scenario for this century, given an 11% reduction in precipitation, runoff is reduced by 13%, while recharge is reduced by only 2%. Conversely, for the PCM A2 model, given a 20% increase in precipitation, runoff is also up by 20%, while recharge is up by 43%. This suggests that during dry years recharge will not suffer as proportionately significant a reduction as runoff, while in wet years there will be a greater benefit in terms of recharge relative to runoff. These results point to the value of sound groundwater management as a climate adaptation strategy.

By focusing on the relationship between soil moisture storage and evapotranspiration pressures, climatic water deficit (CWD) integrates the effects of increasing temperature and variable precipitation on watershed conditions. Our analysis shows under both higher and lower precipitation scenarios for the region, climatic water deficit is projected to increase no matter what, implying greater water demand if maintaining current land cover is a management objective. Our results also show significant differences between major basins in terms of this impact.

In terms of raising awareness regarding the potential impact of climate change on our day-to-day activities, translating climate variability we anticipate over time into terms that people understand based on today's spatial variability may prove an effective approach. For example, a 2 °C difference in average maximum temperatures today creates the differences we experience between the climate of the coast of Marin and the climate of Napa Valley. Such analogies may help to communicate the scope of change that may occur in all of our major basins by mid-century if we stick to "business as usual" greenhouse gas emissions.

Results provided here may be adapted by managers to interface with water supply and to some extent flood management scenarios. The ability to query data down to the scale of sub-basins enables the examination of potential impacts to a specific reservoir or flood management zone. Watershed managers should benefit from an improved understanding the variability of climate resilience or vulnerability within a major planning basin when evaluating site-specific project alternatives.

To improve water supply and flood vulnerability assessments, we recommend that managers consider further downscaling these tools to daily time intervals (a project currently underway by the USGS for the Russian River basin) to generate statistically meaningful estimates of recurrence probabilities for extremes including drought and floods that are contingent on daily hydrologic variations.

These climate projections underscore the importance of implementing long-term watershed monitoring programs to evaluate hydrologic parameters in “real time” as we move forward into an uncertain future (Ridolfi and others 2010). Empirical measurements of watershed response to variations in climate combined with applied management strategies will be crucial to effective adaptive watershed management in the decades to come.

Acknowledgments

The authors acknowledge the North Bay Watershed Association for core project funding, and US Geologic Survey, Bay Area Open Space Council, Pepperwood Foundation, Creekside Center for Earth Observation, and Switzer Foundation for supplemental support. We are also grateful to colleagues who provided input on previous drafts of this study.

References

- Bouwer LM, Aerts JC, Van de Coterlet GM, Van de Giesen N, Gieske A, Mannaerts C. 2004. Evaluating downscaling methods for preparing global circulation model (GCM) data for hydrological impact modeling: *in* Climate Change in Contrasting River Basins (eds. Aerts JC, Droogers P), CAB International Publishing, London, UK, p. 25-47.
- CalWater. 1999. California Interagency Watershed Map of 1999 (CalWater Version 2.2.1). Prepared by the Natural Resources Conservation Service California Interagency Watershed Mapping Committee. <http://www.ca.nrcs.usda.gov/Features/calwater>.
- Cayan DR, Maurer EP, Dettinger MD, Tyree M, Hayhoe K. 2007. Climate change scenarios for the California region. Climatic Change. DOI 10.1007/s10584-007-9377-6.
- Cayan DR, Tyree M, Dettinger MD, Hidalgo H, Das T. 2009. California climate change scenarios and sea level rise estimates for the California 2008 Climate Change Scenarios Assessment. California Energy Commission Report No. CEC-500-2009-014-F. <http://www.energy.ca.gov/2009publications/CEC-500-2009-014/CEC-500-2009-014-F.PDF>
- Cornwell W. 2010. Ackerly Lab, Department of Integrative Biology, UC Berkeley, personal communication. <http://www.zoology.ubc.ca/~cornwell/>
- Daly C, Gibson WP, Doggett M, Smith J, Taylor G. 2004. Up-to-date monthly climate maps for the conterminous United States. Proc., 14th AMS Conf. on Applied Climatology, 84th AMS Annual Meeting Combined Preprints, Amer. Meteorological Soc., Seattle, WA, January 13-16, 2004, Paper P5.1, CD-ROM. http://www.prism.oregonstate.edu/pub/prism/docs/appclim04-uptodate_monthly_climate_maps-daly.pdf
- Delworth TL and others. 2006. GFDL's CM2 global coupled climate models—Part 1: Formulation and simulation characteristics, J. Clim., 19, 643– 674.
- Flint AL, Flint LE. 2007a. Application of the Basin Characterization Model to estimate in-place recharge and runoff potential in the Basin and Range carbonate-rock aquifer system, White Pine County, Nevada, and adjacent areas in Nevada and Utah. U.S.

Geological Survey Scientific Investigations Report 2007-5099.

<http://pubs.water.usgs.gov/sir20075099>

Flint LE and Flint AL in Stonestrom DA, Constantz J, Ferré TPA and Leake SA (eds). 2007b. Ground-Water Recharge in the Arid and Semiarid Southwestern United States. Professional Paper 1703. U.S. Geological Survey, Reston, Virginia.

<http://pubs.usgs.gov/pp/pp1703/pp1703>

Flint LE and Flint AL. 2011. Downscaling future climate scenarios to fine scales for hydrologic and ecologic modeling and analysis. (*unpublished manuscript in review*)

Hidalgo H, Dettinger MD, and Cayan DR. 2008. Downscaling with constructed analogues- Daily precipitation and temperature fields over the United States. California Energy Commission Report No. CEC-500-2007-123.

http://meteora.ucsd.edu/cap/pdf/files/analog_pier_report.pdf

[IPCC] Intergovernmental Panel on Climate Change. 2001. Climate change 2001, the third assessment report (AR3) of the United Nations Intergovernmental Panel on Climate Change.

http://www.ipcc.ch/publications_and_data/publications_and_data_reports.htm

[IPCC] Intergovernmental Panel on Climate Change. 2007. Climate Change 2007, the fourth assessment report (AR4) of the United Nations Intergovernmental Panel on Climate Change.

http://www.ipcc.ch/publications_and_data/publications_and_data_reports.htm

Knowles N, Cayan D. 2002. Potential effects of global warming on the Sacramento-San Joaquin watershed and the San Francisco Estuary. Geophysical Research Letters 29:38-1-38-4. http://tenaya.ucsd.edu/~knowles/papers/knowles_grl_2002.pdf

Loarie SR, Ackerly DD. 2004. The distribution of California's endangered plants in multivariable climate space. 6th Annual Bay Area Conservation Biology Symposium.

Meehl GA, Washington WM, Wigley TML, Arblaster JM, Dai A. 2003. Solar and greenhouse gas forcing and climate response in the twentieth century. J Climate 16(3): 426-444.

Nakic'enovic' N, Alcamo J, Davis G, de Vries B, Fenhann J, Gaffin S, Gregory K, Grubler A, Jung TY, Kram T. 2000. Intergovernmental panel on climate change special report on emissions scenarios. Cambridge Univ. Press, Cambridge, U.K

Nalder IA, Wein RW. 1998. Spatial interpolation of climatic normals: Test of a new methods in the Canadian boreal forest. Agricultural and Forest Meteorology 92: 211-225.

North Bay Watershed Association (NBWA). 2003. North Bay Watershed Stewardship Plan. Novato, CA.

NRCS (Natural Resources Conservation Service). 2006. U.S. General Soil Map (STATSGO2). http://www.ftw.nrcs.usda.gov/stat_data.html,
<http://soils.usda.gov/survey/geography/statsgo/description.html>.

Ridolfi K, Vorster P, Micheli L. 2010. *Indicators and Performance Measures for North Bay Watersheds*. Prepared for the North Bay Watershed Association by the San Francisco Estuary Institute. Alameda, CA. 36 pp.

Stephenson NL. 1998. Actual evapotranspiration and deficit: Biologically meaningful correlates of vegetation distribution across spatial scales: *Journal of Biogeography*, Vol. 25, No. 5, pp. 855-870.

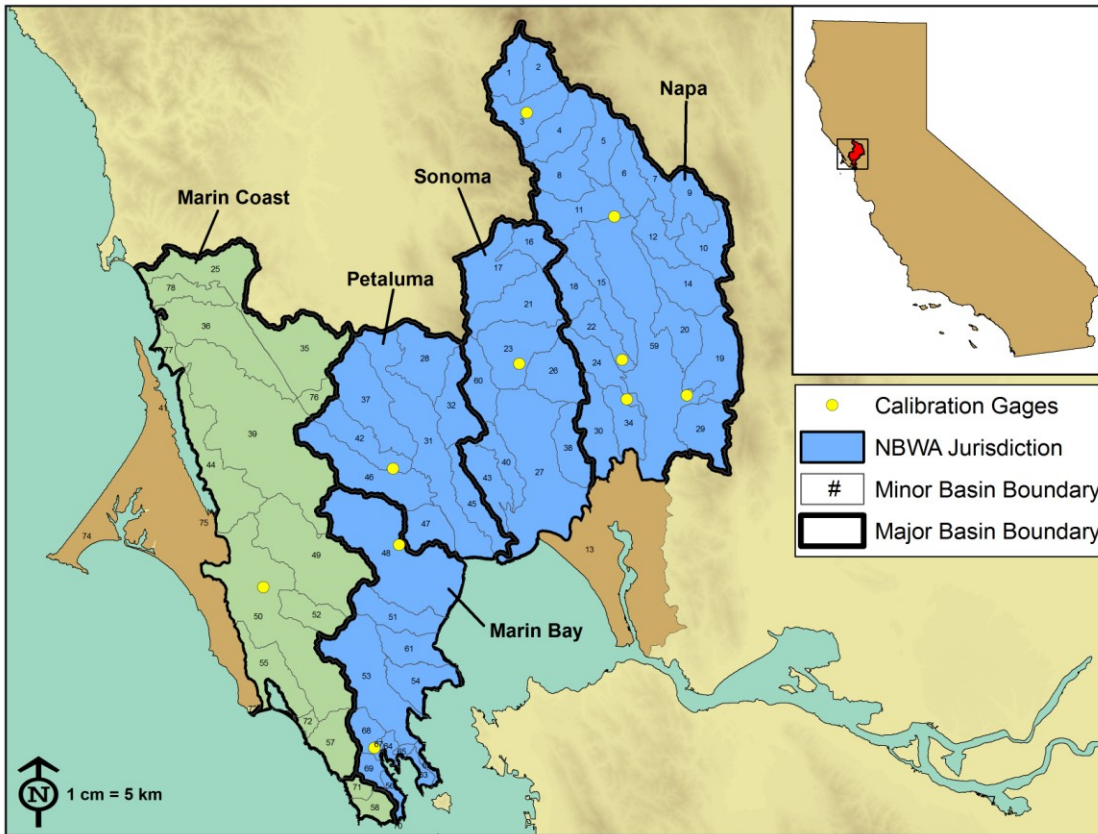
Stouffer RJ and others. 2006. GFDL's CM2 global coupled climate models – Part 4: Idealized climate response. *J Climate* 19: 723–740.

Washington WM, Weatherly JW, Meehl GA, Semtner AJ, Bettge TW, Craig AP, Strand WG, Arblaster J, Wayland VB, James R, and Zhang Y. 2000. *Clim Dyn* 16 (10/11): 755–774.

Weiss SB, Schaefer N, Branciforte R. 2007. *Upland Habitat Goals: Study Design and Methodology*. Prepared for Bay Area Open Space Council, Berkeley, CA. 33 pp.

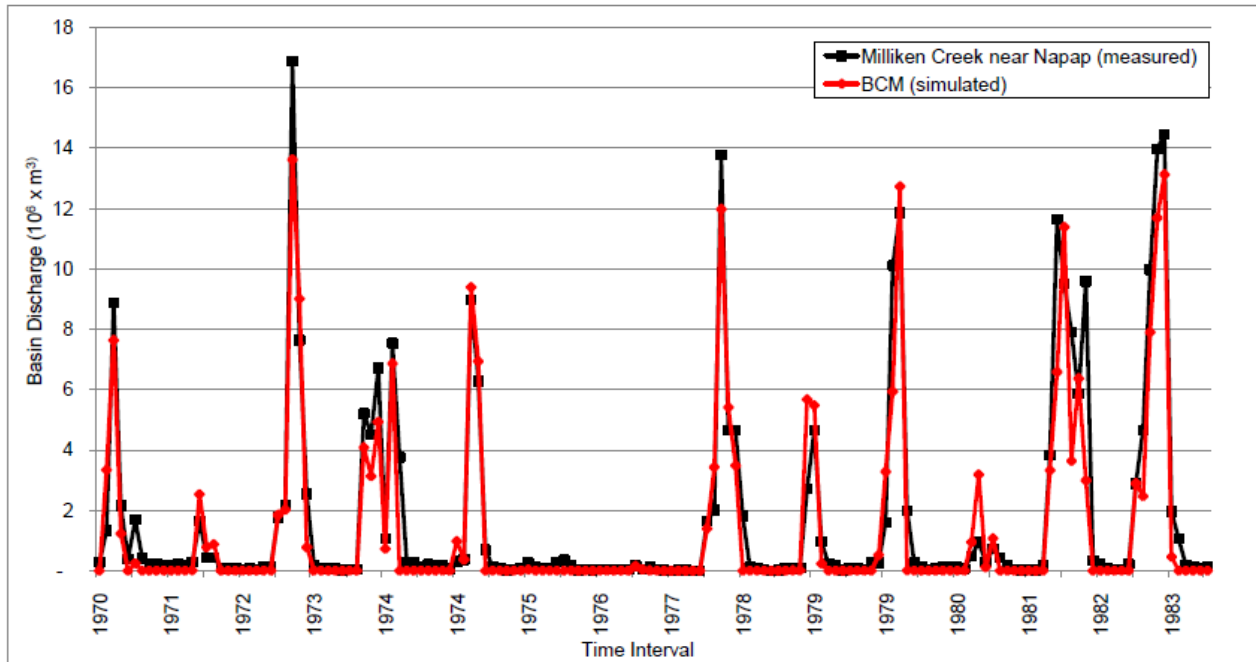
**Downscaling future climate scenarios to the watershed scale:
a North San Francisco Bay Estuary case study**
FIGURES and TABLES

Figure 1 Site Location



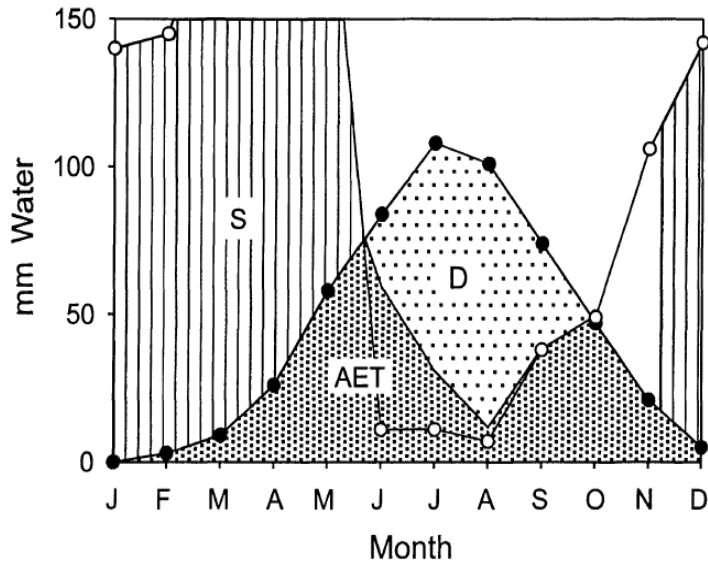
Map of study area delineating major and minor basins analyzed using Basin Characterization Model (BCM). Blue shading defines North Bay Watershed Association (NBWA) jurisdiction which we term “North Bay region” for this study. Labels with arrows identify major basins. Small numbers label minor basins identified by name in Appendix A. Yellow circles show location of USGS gages used for model calibration listed in Table 1.

Figure 2 Model calibration example: comparison of modeled and measured monthly stream discharge, Milliken Creek, Napa River basin, 1970-1983



Monthly stream discharge measured at the USGS gage 11458100 (Milliken Creek near Napa) in black (square labels) compared to Basin Characterization Model (BCM) stream discharge measurements in red (diamond labels) produced via calibration run. Each gage shown in Figure 1 was used for model calibration to ensure the BCM effectively captures magnitude and timing of peaks in monthly discharge.

Figure 3 Climatic water deficit



Climatic water deficit quantifies evaporative demand exceeding available soil moisture, where S = soil moisture, AET = actual evapotranspiration, D = climatic water deficit. After Stephenson 1998.

Figure 4A-C Average annual precipitation and maximum and minimum temperatures, North Bay region, 1971-2000

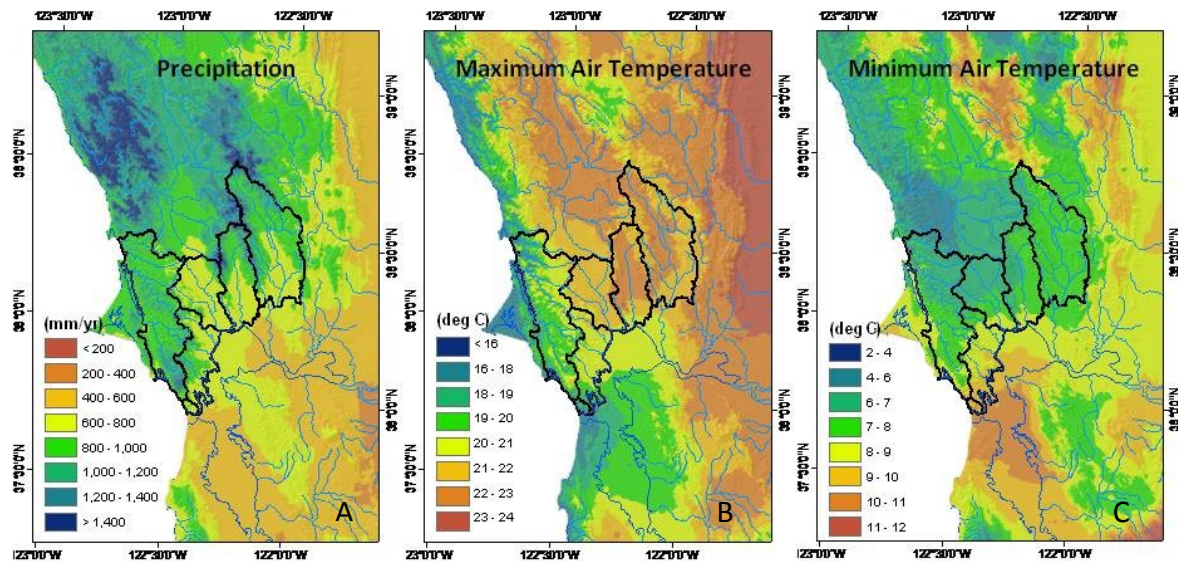
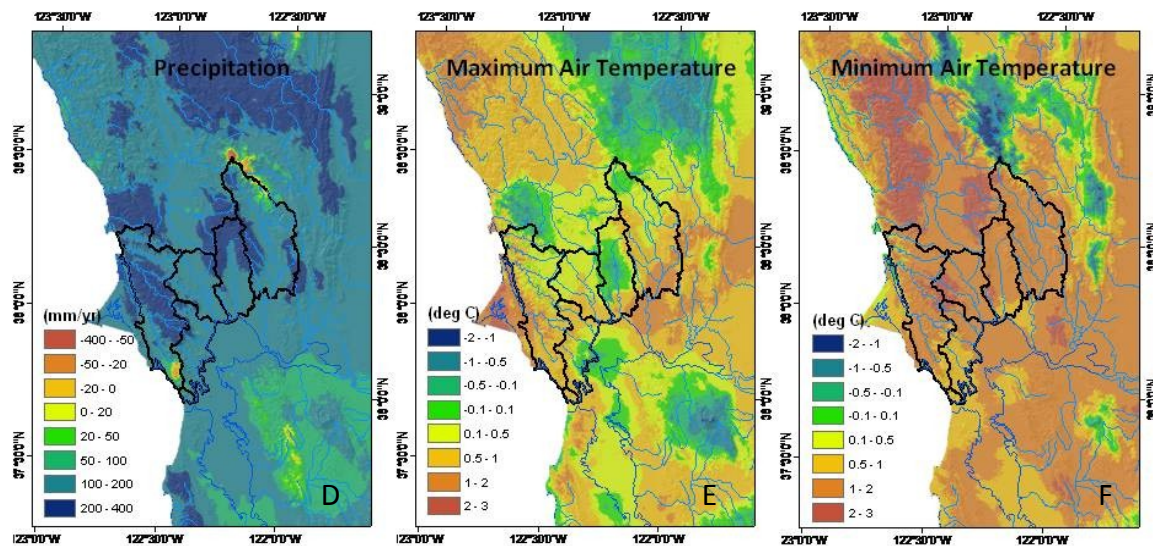


Figure 4D-F Direction and magnitude of change in annual average precipitation and maximum and minimum temperatures, North Bay region, 1971-2000



Trend analysis for precipitation and temperature across North Bay region based on based on monthly PRISM data downscaled to 270 m for 1971-2000. Series A-C shows average annual values and series D-F shows total change for this time period. Major basins are delineated in black outline. A-C display a decreasing precipitation gradient from the coast and montane headwaters to inland valleys, an increasing gradient in maximum temperatures from coast (18-19 °C) to inland (22-23 °C), and relatively consistent trends across the region in minimum temperatures. D-E display an increase of approximately 50-200 mm in precipitation, a variable trend in maximum temperatures, and more intensive increases in minimum temperature (on the order to 1-2 °C) across the region.

Figure 5A Historic (1901-2000) and GCM-projected (2001-2100) maximum temperatures

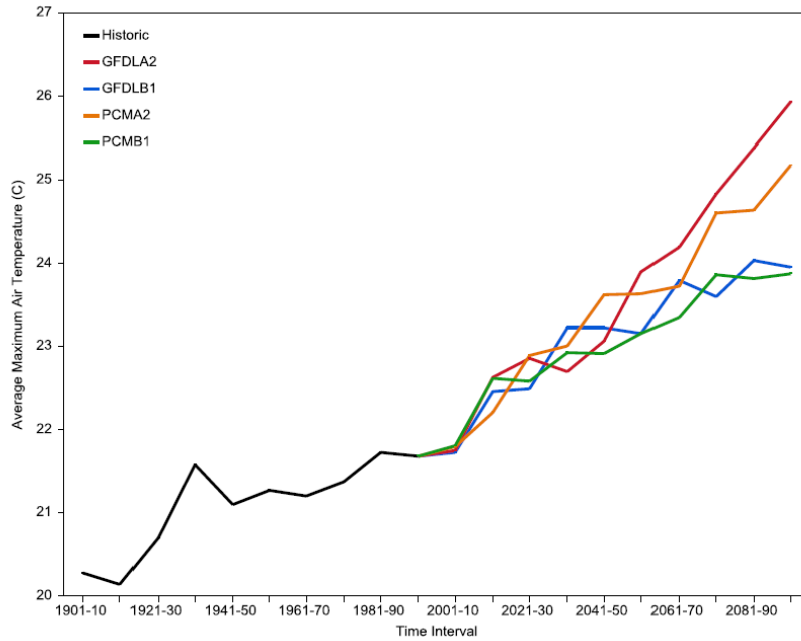
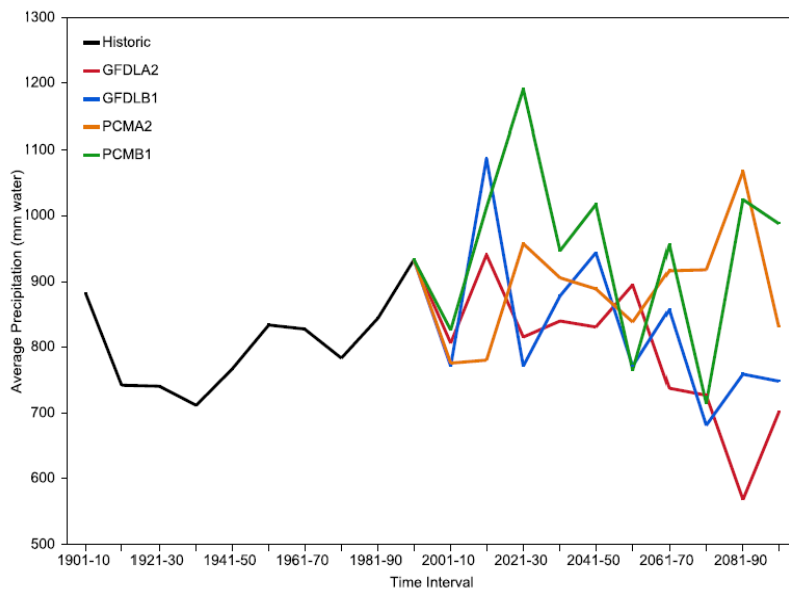
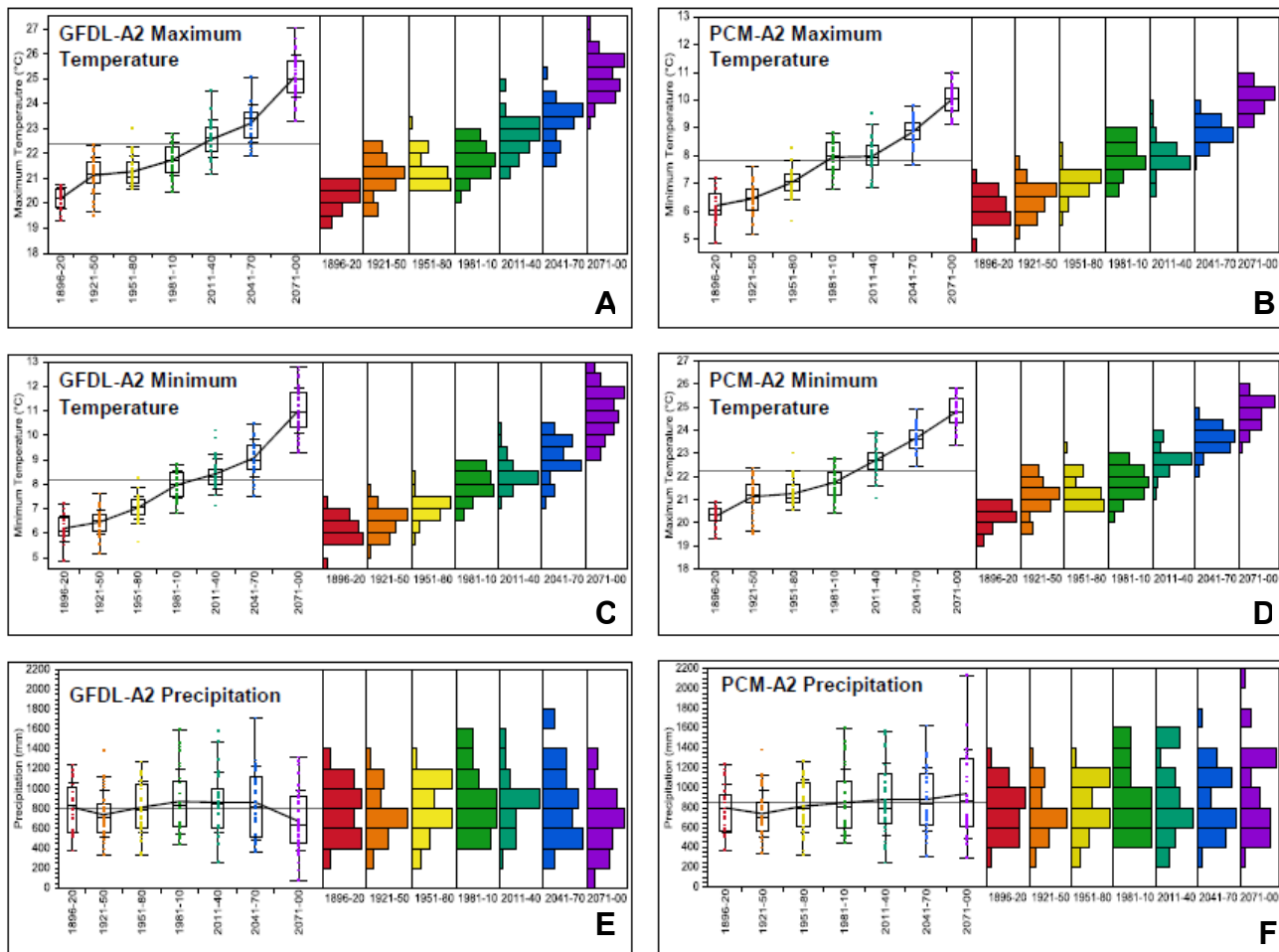


Figure 5B Historic (1901-2000) and GCM-projected (2001-2100) precipitation



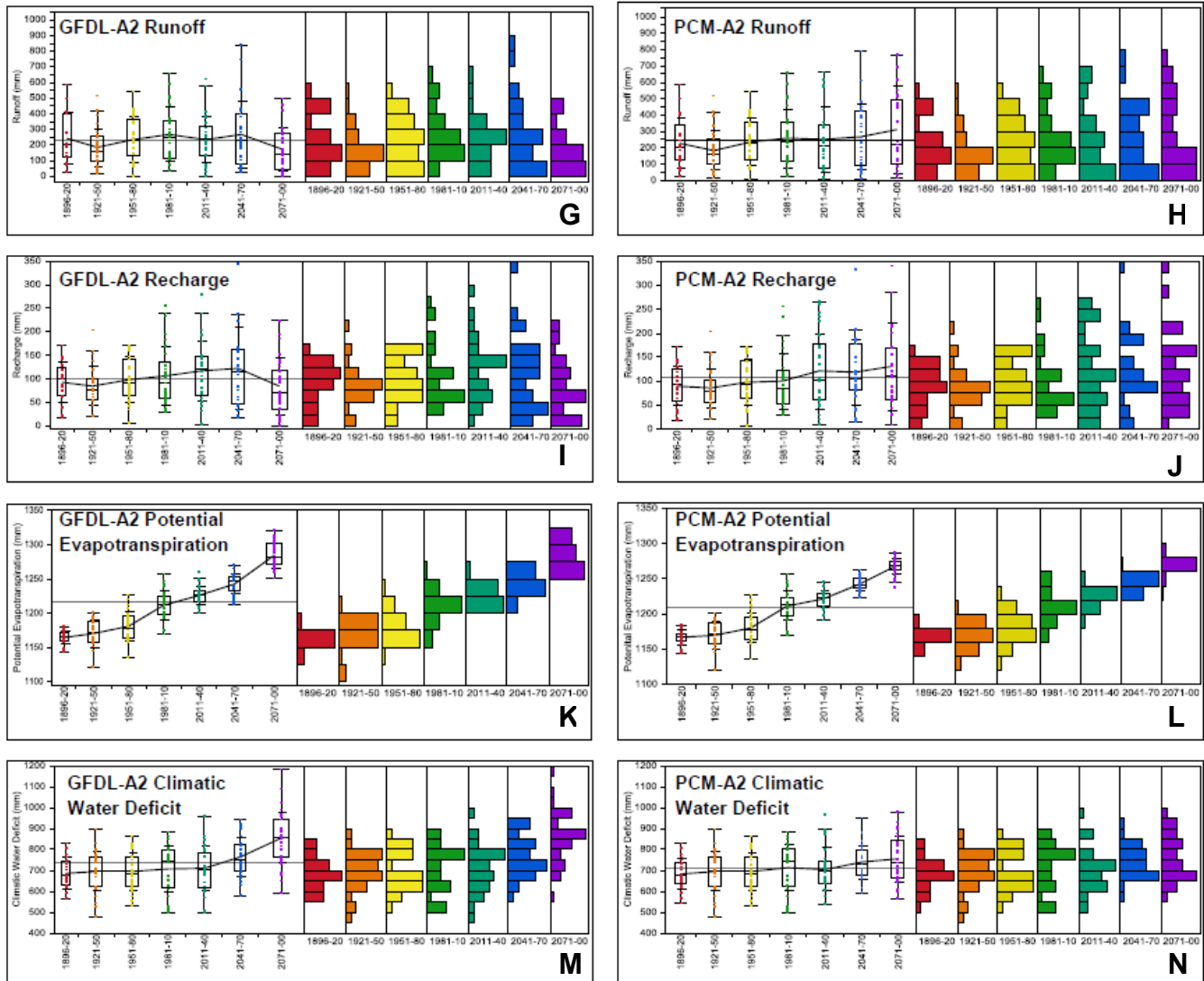
General Circulation Model (GCM) temperature and precipitation outputs downscaled to North Bay region based on monthly values averaged over decade intervals. Historic values derived from PRISM. Projected data series (2001-2100) represent four combinations of GCM model (GFDL or PCM) and emissions scenario (A2 “business as usual”, B1 “mitigated”) as identified in legend.

Figure 6A-F Historic (1896-2009) and projected (2010-2100) temperature and precipitation, North Bay region, GFDL A2 and PCM A2 scenarios



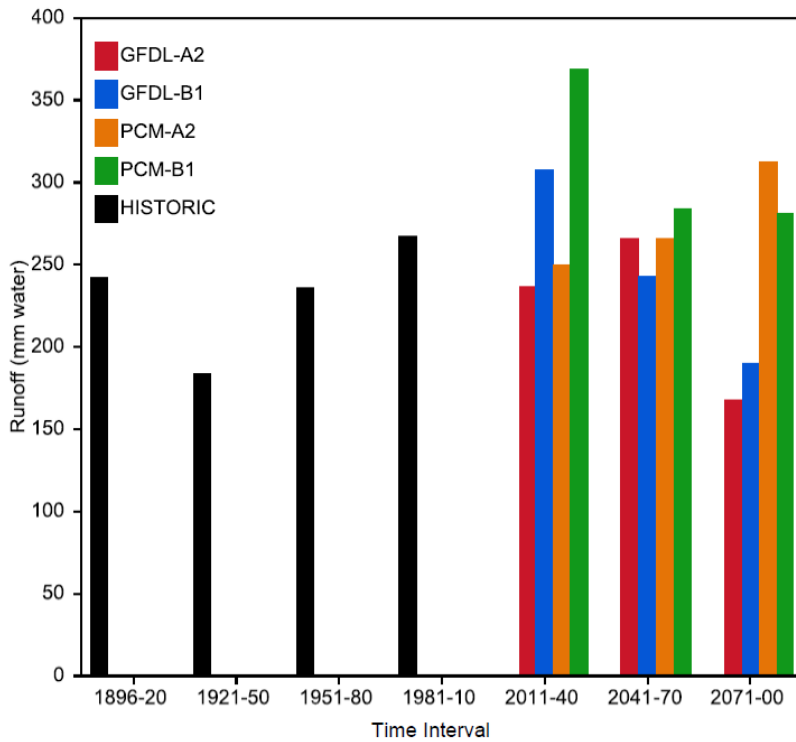
Historic values (1896-2009) for temperature and precipitation derived from PRISM, projected values for temperature and precipitation derived from downscaled GCMs (GFDL A2 “warmer drier” and PCM A2 “warmer wetter” scenarios, 2010-2100). Box plots represent 30-year intervals and are sized to the standard deviation, “whiskers” define the 5-95% confidence interval, and histograms show the frequency distributions of average annual values.

Figure 6G-N Historic (1896-2009) and projected (2010-2100) hydrology, BCM estimates, North Bay region, GFDL-A2 and PCM A-2 scenarios



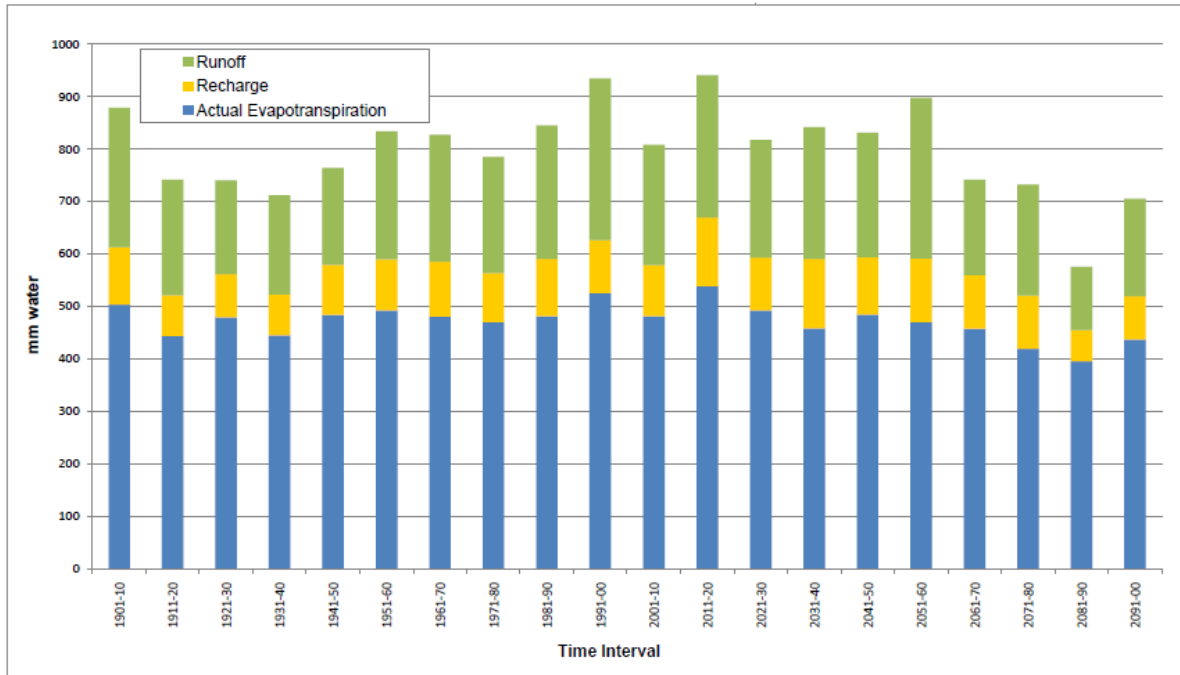
Hydrologic parameters of runoff (G-H), recharge (I-J), evapotranspiration (K-L), and water deficit (M-N) are derived from Basin Characterization Model (BCM) simulations using PRISM data for historic values (1896-2009) and using downscaled GCMs (GFDL A2 “warmer drier” (G, I, K, M) and PCM A2 “warmer wetter” (H, J, L, N) for future projections (2010-2100). Box plots represent 30-year intervals and are sized to the standard deviation, “whiskers” define the 5-95% confidence interval, and histograms show the frequency distributions of average annual values.

Figure 7 A comparison of historic (1896-2009) to projected (2010-2100) average annual runoff for four future climate scenarios, North Bay region



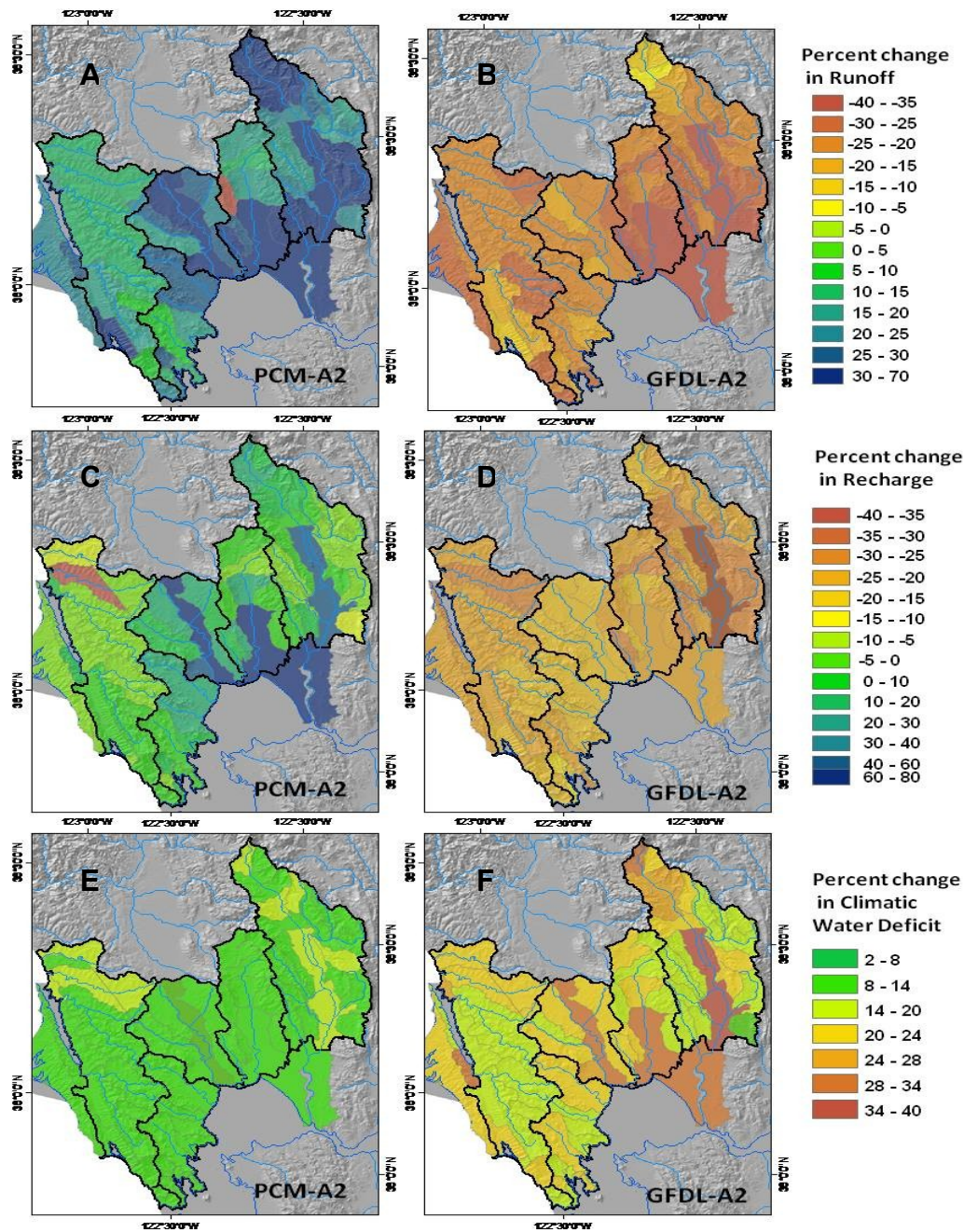
Each bar represents average annual runoff estimated by the Basin Characterization Model (BCM) for the North Bay region (NBWA jurisdiction) over the defined time interval, with black bars derived from PRISM data (1896-2009) and colored bars derived from GCM projections. For the three projected time periods, the first (2011-2040) shows a case where the B1 scenarios are significantly wetter than the A1 scenarios, the second (2041-2070) shows a case where all scenarios are comparable in terms of projected runoff, while the third (2071-2100) demonstrates a case where the PCM projections are significantly wetter than the GFDL projections for both emissions scenarios.

Figure 8 Historic (1896-2009) versus projected (2010-2100) water balance partitioning, North Bay region



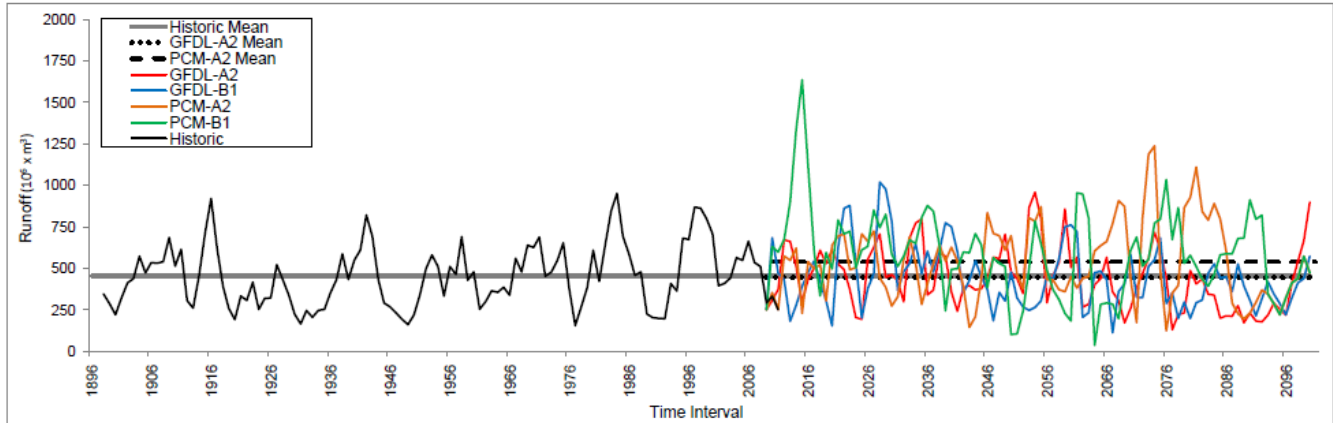
This plot shows estimated water balance distributions for the historic period (1896-2009) and GFDL A2 “warmer drier” scenario (2010-2100) using monthly data averaged over decade intervals. Histograms displaying water balance partitioning between runoff (green), recharge (yellow) and evapotranspiration (blue) show that in low water years proportionally more water is converted to evapotranspiration versus during high water years when proportionally more water is available for recharge and runoff.

Figure 9A-F Spatial distribution of projected climate impacts on hydrology estimated using Basin Characterization Model (BCM), North Bay region



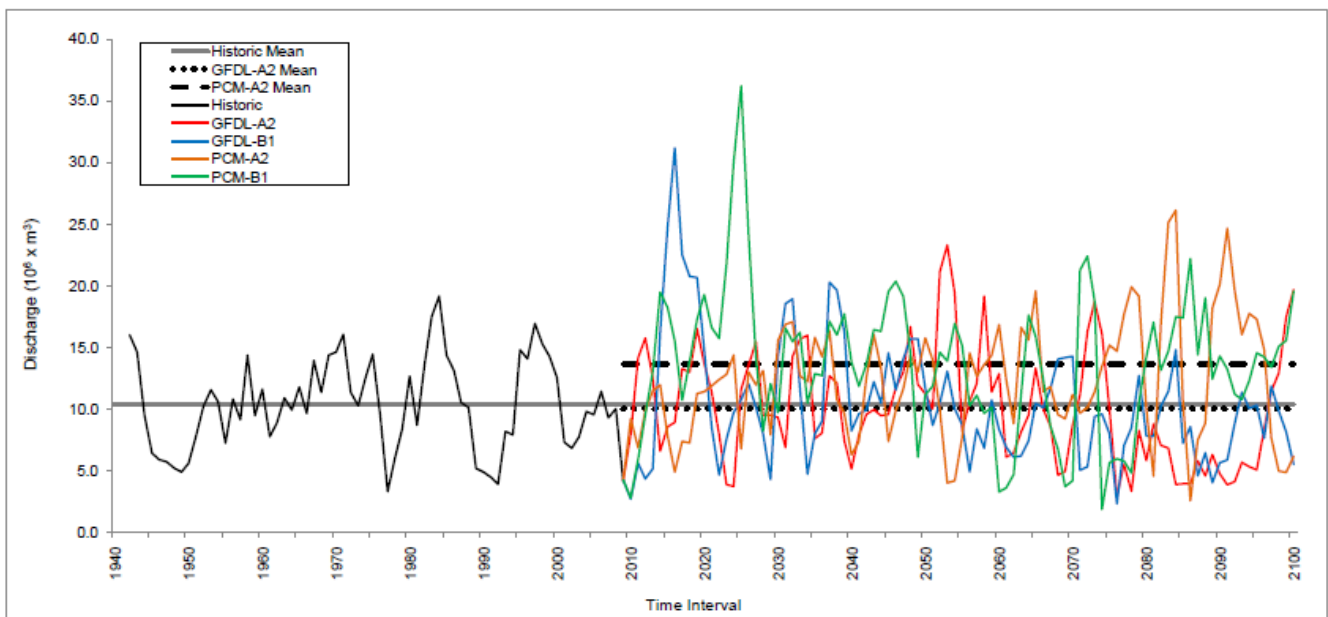
Maps A-F display the diversity of potential hydrologic response to climate change within major basins by showing the spatial distribution of differences between the 1971-2000 and 2071-2100 time intervals. A-B displays runoff, C-D displays recharge, and E-F displays water deficit for the PCM A2 “warmer wetter” scenario (A, C, E) and the GFDL A2 “warmer drier” scenario (B, D, F). 270 m grid results are averaged for sub-basins. In general, valley bottoms typified by thick layers of alluvium show the greatest magnitude of potential change due to storage capacity. While runoff and recharge generally trend in opposite directions for the two models (in the positive direction for PCM and the negative direction for GFDL), both models predict increases in water deficit ranging from 8 to greater than 34%.

Figure 10A Historic (1896-2009) and projected (2010-2100) runoff, three-year running average, North Bay region



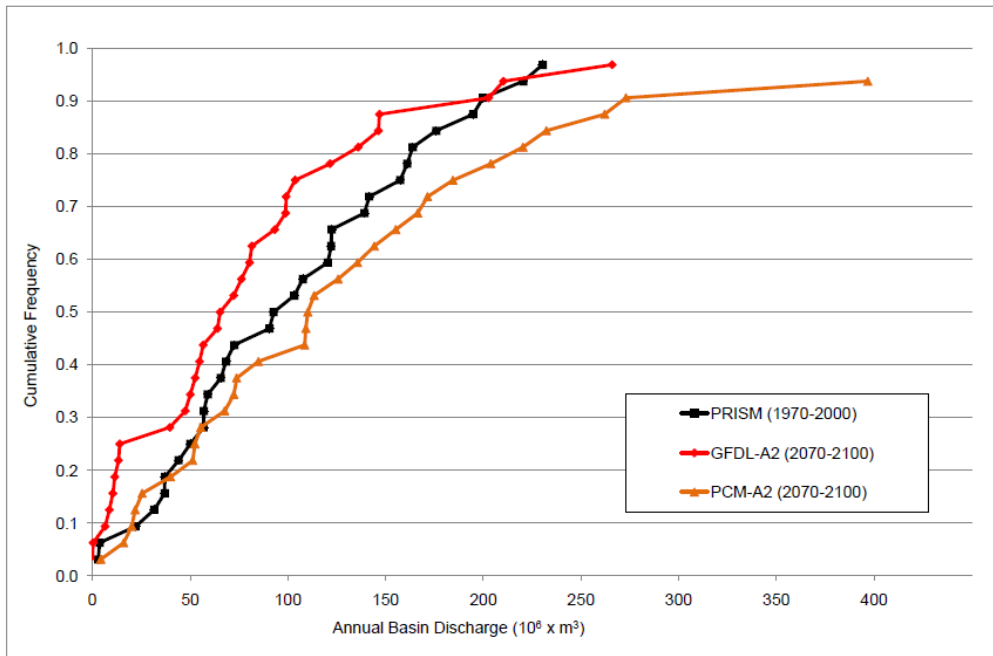
Historic estimated runoff (1896-2009, derived from PRISM data) and projected runoff (2010-2100) for four scenarios (PCM A2 in yellow, GFDL A2 in red, PCM B1 in green, GFDL B1 in blue) for North Bay region (excludes Marin Coast planning basin). Plot shows increased future variability in three-year running average for all scenarios. Trend lines display historic mean (solid), PCMA 2 mean (dashed), and GFDL A2 mean (dotted) values over respective time periods.

Figure 10B Historic (1896-2009) and projected (2010-2100) stream discharge, three-year running average, Napa River at St Helena



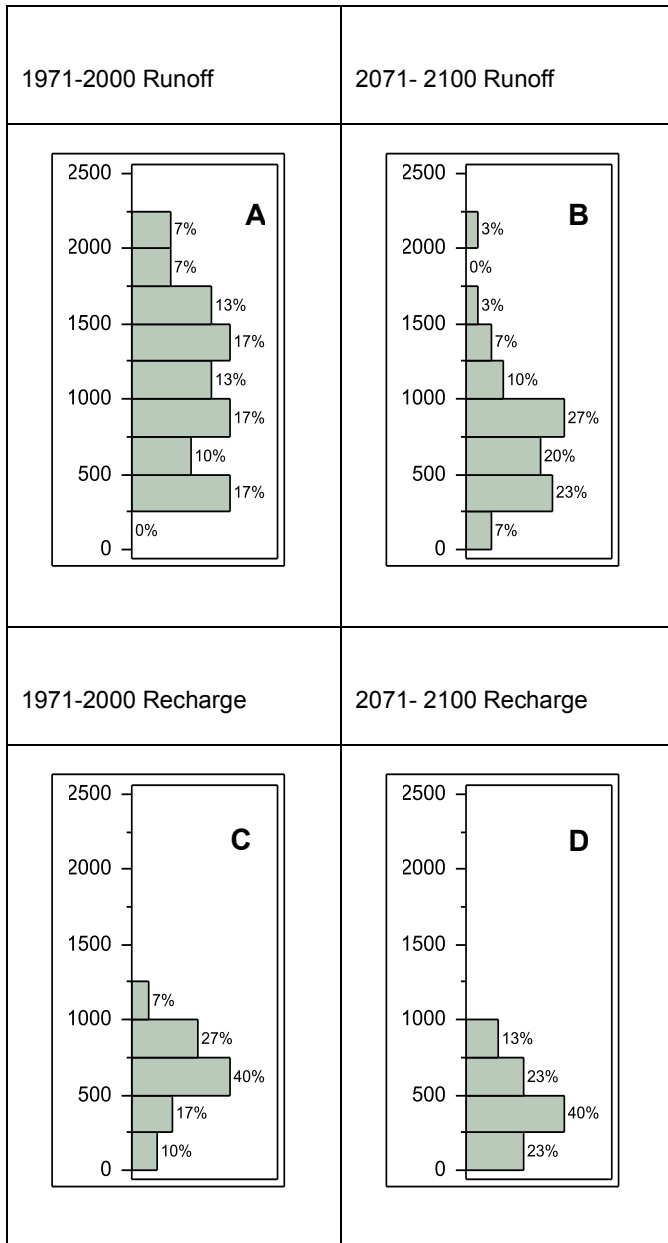
Historic stream discharge (1896-2009, derived from USGS gage data) and projected stream discharge for four scenarios (PCM A2 in yellow, GFDL A2 in red, PCM B1 in green, GFDL B1 in blue) for USGS gage on Napa River at St Helena, #1145600. Plot displays increased future variability in 3-year running average for all scenarios, and trend towards end of current century for more discharge under PCM compared to GFDL scenarios. Trend lines display historic mean (solid), PCM A2 mean (dashed), and GFDL A2 mean (dotted) values.

Figure 11 Historic (1971-2000) versus projected (2071-2100) cumulative probability of annual stream discharge, Napa River at St Helena



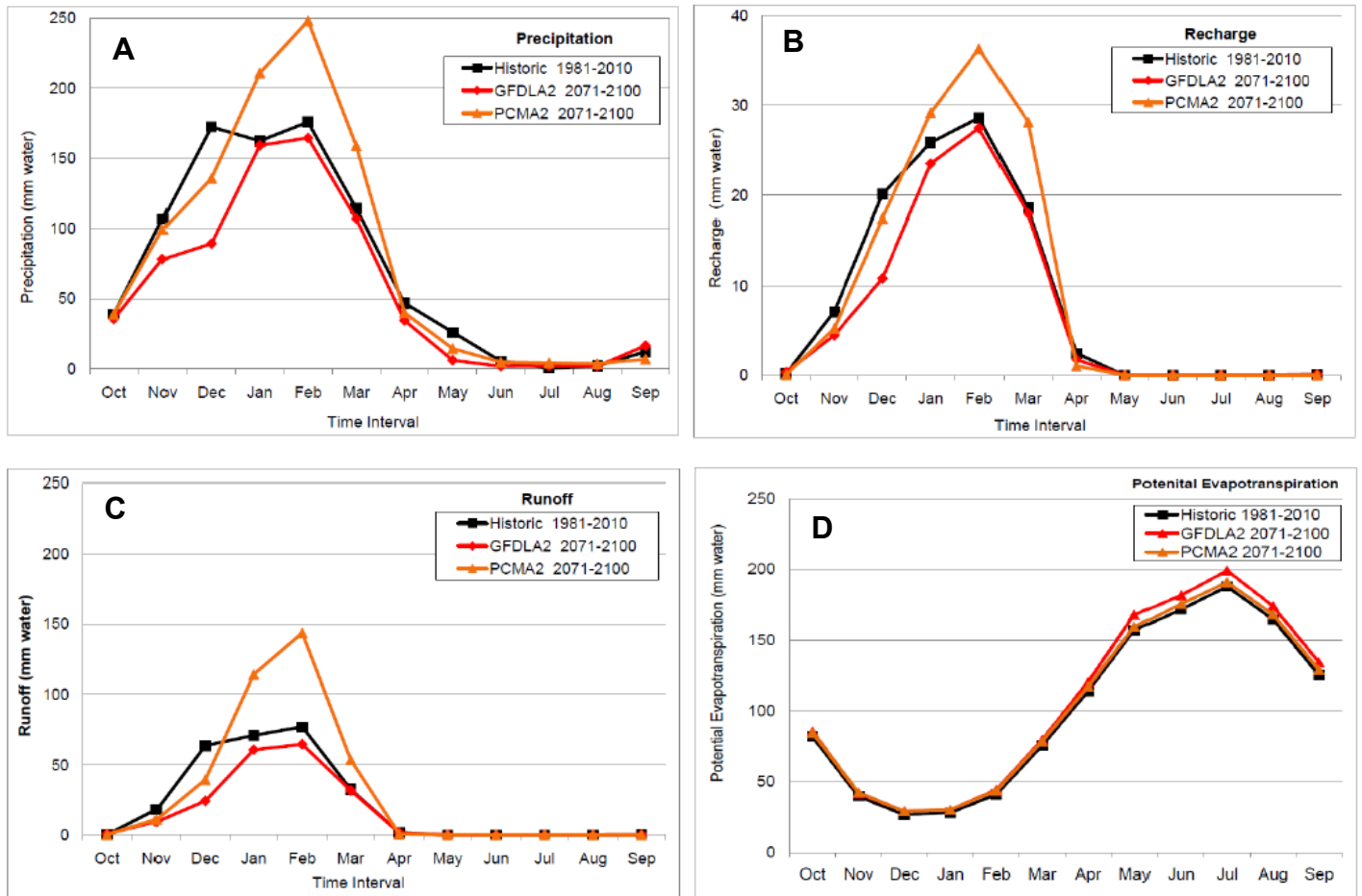
Annual basin discharge versus cumulative frequency for the Napa River at St Helena, where black squares represent historic conditions (1971-2000, derived from USGS gage data), red diamonds represent projected GFDL A2 scenario (2071-2100, BCM simulation), and gold triangles represent projected PCM A2 scenario (2071-2100, BCM simulation).

Figure 12A-D Runoff and recharge, three-year running average values, historic (1971-2000) and GFDL-A2 projections GFDL-A2 (2071-2100), Milliken Creek sub-basin



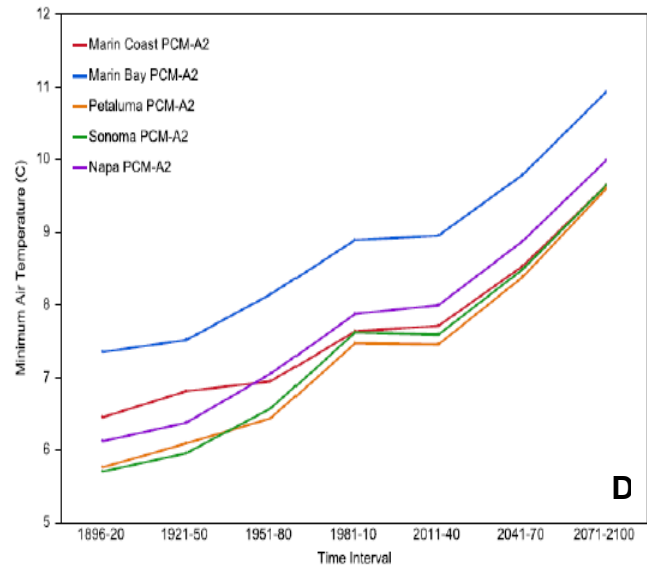
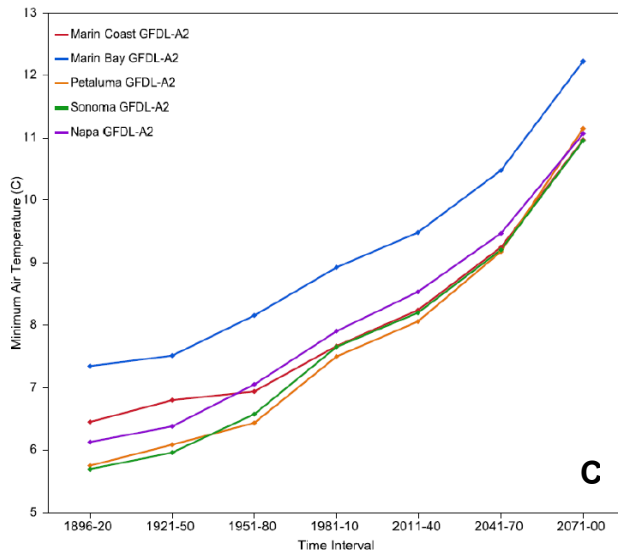
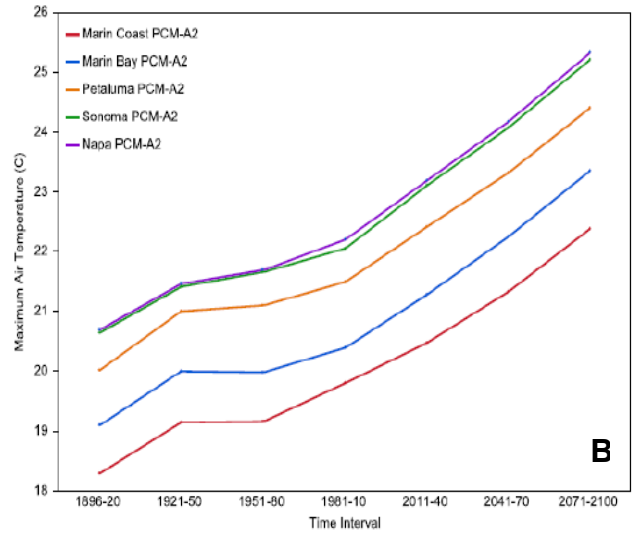
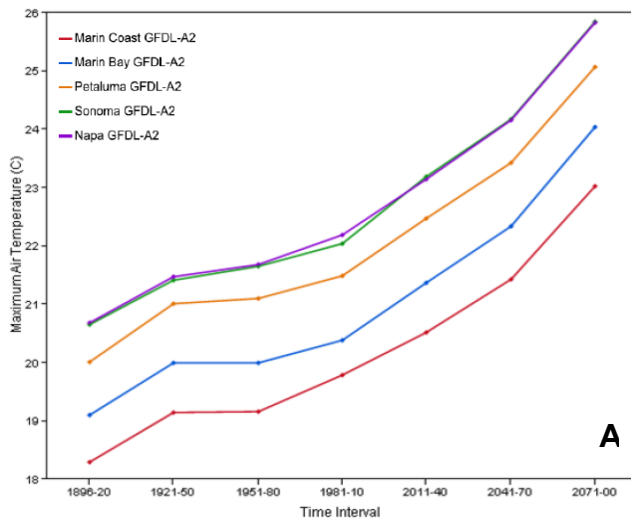
Histograms compare frequency distributions for 1971-2000 (derived from USGS gage data) and 2071-2100 (derived from BCM simulation for GFDL-A2 scenario) in terms of three-year running average values for runoff (A-B) and recharge (C-D). Percent labels show total frequency of values for each histogram interval. Units are $10^3 \times m^3$ of water.

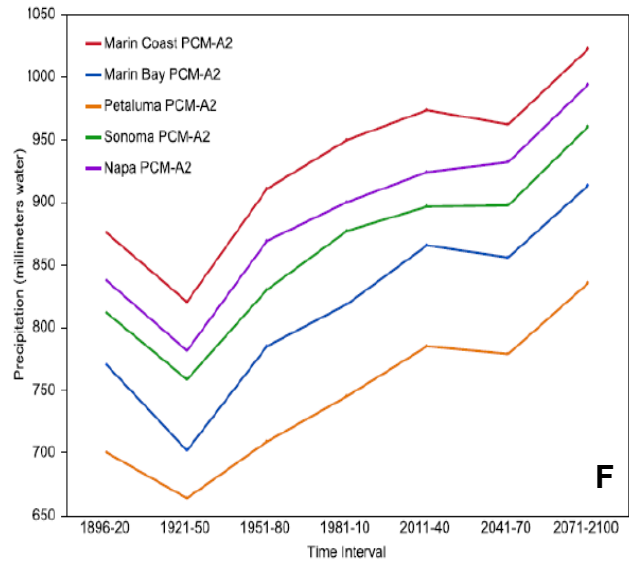
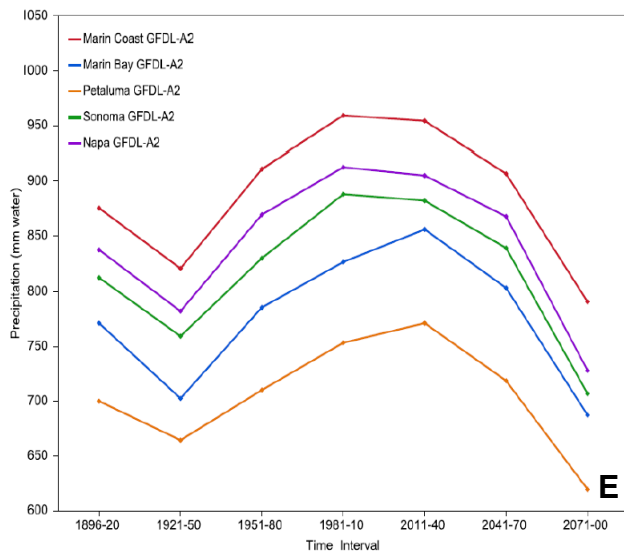
Figure 13A-D Projected climate impacts on seasonality of climate hydrology parameters, North Bay region



Each plot compares recent (1981-2010) versus projected (2071-2100) monthly average values for individual months of water year for A) precipitation, B) runoff, C) recharge, and D) potential evapotranspiration. Black squares show recent values (derived from PRISM), red diamonds shows projected “warmer-drier” scenario (GFDL A2 scenario, 2071-2100, BCM simulation), gold triangles show “warmer-drier” (PCM A2 scenario, 2071-2100, BCM simulation). Although the PCM A2 model projects unprecedented amounts of precipitation during winter months, it also projects lower water availability by April compared to current conditions. The GFDL A2 model projects significantly less water available in both the early and late months of wet season compared to current conditions.

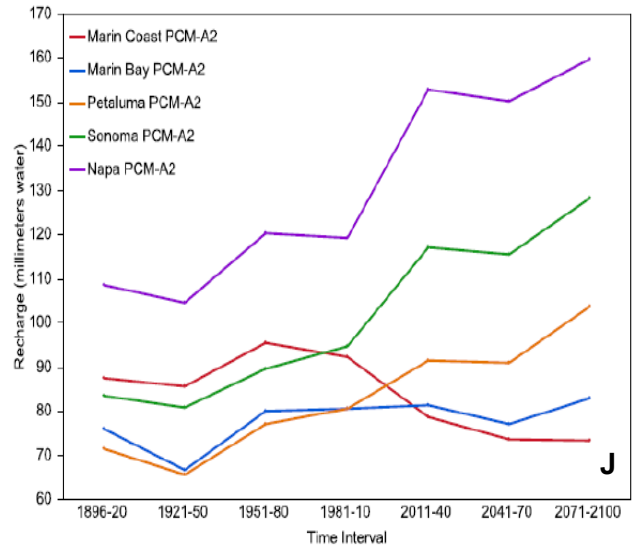
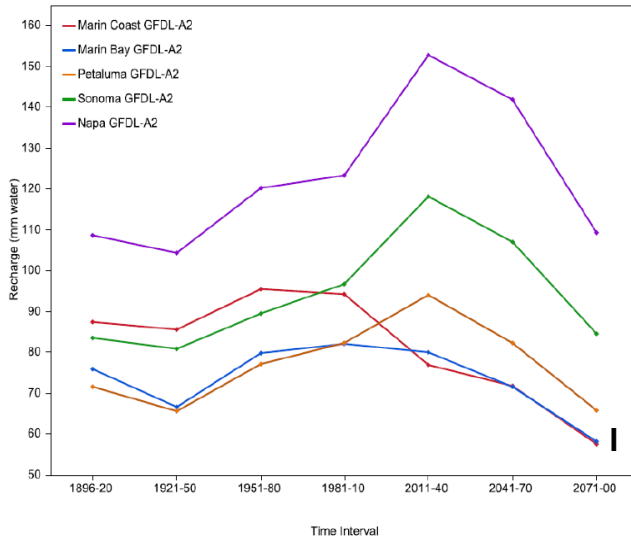
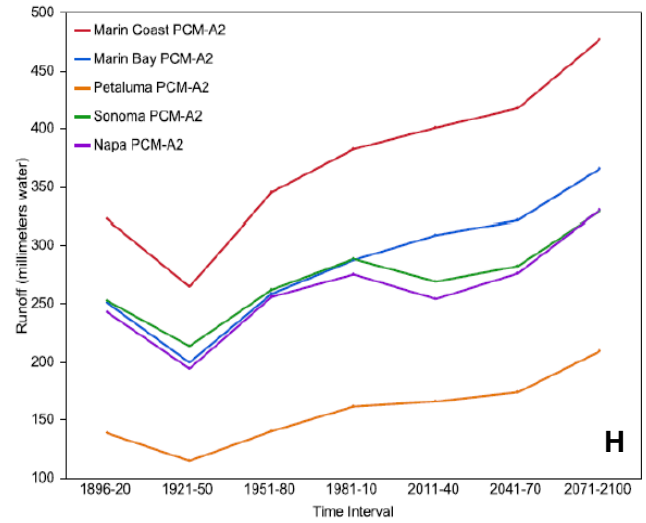
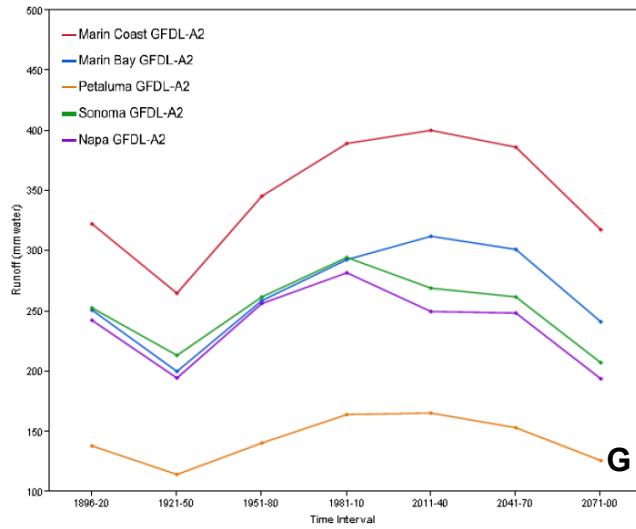
Figures 14A-F Historic (1896-2009) and projected (2010-2100) maximum and minimum temperatures and precipitation by major basin, North Bay region, GFDL-A2 and PCM-A2 scenarios

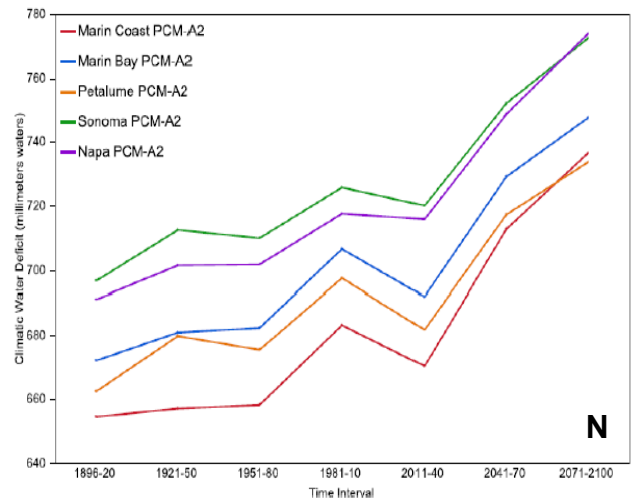
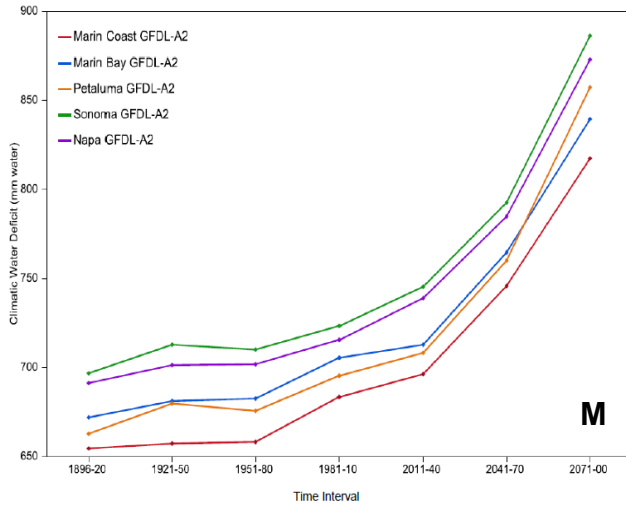
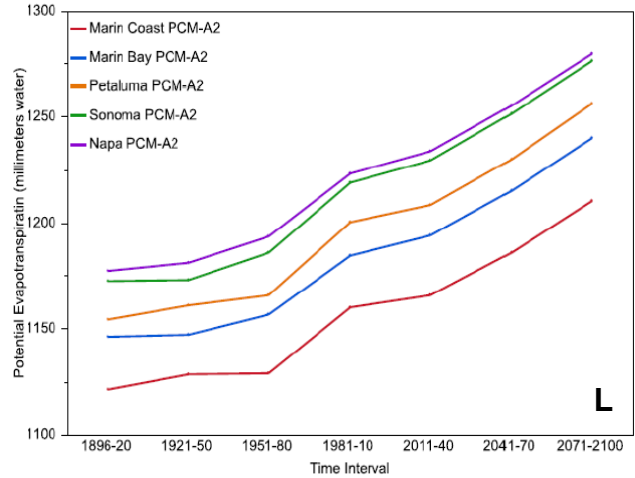
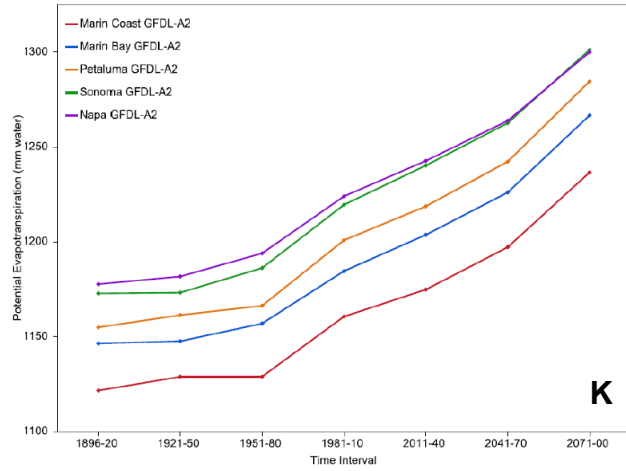




Plots compare major basin attributes for maximum temperatures (A-B), minimum temperatures (C-D) and precipitation (E-F) for GFDL A2 and PCM A2 scenarios. Marin Coast shown in purple, Marin Bay shown in blue, Petaluma River basin shown in red, Sonoma Creek basin shown in green, and Napa River basin shown in gold. Appendix B displays results in tabular form.

Figures 14G-N Historic (1896-2009) and projected (2010-2100) hydrology by major basin, North Bay region, GFDL-A2 and PCM-A2 scenarios





Plots compare major basin attributes for runoff, recharge, potential evapotranspiration, and water deficit for GFDL A2 and PCM A2 scenarios. Marin Coast shown in purple, Marin Bay shown in blue, Petaluma River basin shown in red, Sonoma Creek basin shown in green, and Napa River basin shown in gold. Appendix B displays results in tabular form.

Table 1 Stream gages used for Basin Characterization Model calibration

Gage	USGS#	Period of Record	Ratio of Measured to Modeled Runoff
Napa River Near St Helena	11456000	1975-1983	0.983
Novato Creek at Novato	11459500	1960-1990	0.990
Sonoma Creek at Agua Caliente	11458500	1960-1980	0.994
San Antonio Creek near Petaluma	11459300	1975-1981	1.007
Milliken Creek near Napa	11458100	1970-1983	1.009
Dry Creek near Napa	11457000	1959-1966	0.988
Napa River at Calistoga	11455900	1975-1982	0.996
Arroyo Corte Madera at Mill Valley	11460100	1965-1985	1.009

Table 2 Monthly measured climate and simulated hydrologic parameters (1901-2010), averaged per decade

Decade	Maximum air temperature*		Minimum air temperature*		Precipitation*		Runoff**		Recharge**		Potential evapo-transpiration**		Climatic water deficit**	
	°C	SE	°C	SE	mm y-1	SE	mm y-1	SE	mm y-1	SE	mm y-1	SE	mm y-1	SE
1901-10	20.3	0.3	6.4	0.4	796	237	227	132	97	42	1,234	71	757	127
1911-20	20.1	0.5	5.8	0.4	743	295	220	192	78	50	1,160	9	713	74
1921-30	20.7	0.8	6.4	0.5	742	226	179	96	82	32	1,173	11	689	115
1931-40	21.6	0.6	6.4	0.6	712	240	189	137	78	44	1,174	25	725	72
1941-50	21.1	0.5	6.5	0.5	767	267	185	139	95	48	1,163	21	674	89
1951-60	21.3	0.8	6.9	0.6	834	255	244	157	97	46	1,176	27	679	89
1961-70	21.2	0.6	7.0	0.4	828	229	242	128	105	39	1,178	18	693	91
1971-80	21.4	0.5	7.1	0.5	785	317	221	157	93	61	1,187	18	713	98
1981-90	21.7	0.7	7.5	0.4	845	414	255	220	109	79	1,208	23	723	134
1991-00	21.7	0.8	8.0	0.6	934	318	308	181	101	48	1,212	30	683	96
2001-10	21.8	0.5	8.3	0.3	843	244	245	111	110	64	1,215	6	714	108

* Derived from PRISM climate data (Daly and others,2004)

** Simulated from Basin Characterization Model

Table 3 Four scenarios projected climate and hydrology of North Bay Region study area (2011-2100), monthly values averaged per 30-year interval

Model	Time Interval	Maximum air temperature		Minimum air temperature		Precipitation		Runoff		Recharge		Potential evapo-transpiration		Climatic water deficit	
		oC	SE	oC	SE	mm y-1	SE	mm y-1	SE	mm y-1	SE	mm y-1	SE	mm y-1	SE
Historic*	1921-50	21.1	0.1	6.4	0.1	740	43	184	22	85	8	1,170	4	696	17
	1951-80	21.3	0.1	7.0	0.1	816	48	236	26	98	9	1,181	4	695	17
	1981-10	21.7	0.1	7.9	0.1	874	59	269	32	107	11	1,212	4	707	20
GFDL A2**	2011-40	22.6	0.1	8.4	0.1	864	56	236	27	117	12	1,226	3	710	20
	2041-70	23.2	0.1	9.1	0.1	860	68	266	38	122	16	1,242	3	766	17
	2071-00	25.1	0.1	11.0	0.1	699	54	187	27	89	10	1,286	3	855	19
GFDL B1**	2011-40	22.7	0.1	8.6	0.7	913	84	308	49	132	18	1,228	3	750	19
	2041-70	23.4	0.1	9.2	0.5	858	56	243	32	118	12	1,244	2	742	15
	2071-00	23.9	0.1	9.6	0.5	729	52	189	28	86	11	1,253	2	792	16
PCM A2**	2011-40	22.7	0.1	7.9	0.5	882	67	250	37	121	14	1,221	2	706	19
	2041-70	23.7	0.1	8.9	0.5	882	58	266	36	119	13	1,243	2	740	15
	2071-00	24.8	0.1	10.0	0.5	943	82	313	50	131	17	1,268	2	758	21
PCM B1**	2011-40	22.7	0.1	7.9	0.6	1,051	78	369	45	160	18	1,220	2	692	19
	2041-70	23.1	0.1	8.3	0.5	913	77	284	47	121	16	1,229	2	717	20
	2071-00	23.8	0.1	8.9	0.5	907	65	281	39	120	13	1,243	2	732	18

* Derived from PRISM climate data (Daly and others 2004) and Basin Characterization Model watershed simulations for historic time steps

** Derived from referenced General Circulation Models and Basin Characterization Model watershed simulations

APPENDIX A Major and minor basin descriptors derived from CalWater, 1999

MAJOR BASINS

Major Basin Name	Selected Drainages Included	Area (km2)	Area (acres)
Marin Coast	Lagunitas and San Geronimo Creeks, Bolinas	833.7	206,012
Marin Bay	Miller and Corte Madera Creeks	341.5	84,396
Petaluma River	Stage Gulch Creek	384.9	95,114
Napa River	Conn, York, Milliken, Soda and other Creeks	829.2	204,890
Sonoma Creek	Bear, Calabazas, Carriger, and Nathanson Creeks	431.4	106,593

MINOR BASINS

Minor Basin ID (HRC)	Minor Basin (CalWater CDFPWSNAME)	CalWater HANAME	Major Basin	Area (km2)	Area (acres)
1	Upper Napa River	Napa River	Napa River	24.9	6,165
2	Garnett Creek	Napa River	Napa River	20.6	5,088
3	Simmons Canyon	Napa River	Napa River	34.6	8,560
4	Ritchie Creek	Napa River	Napa River	35.5	8,772
5	Bell Canyon	Napa River	Napa River	27.6	6,830
6	Conn Creek	Napa River	Napa River	29.5	7,297
7	Moore Creek	Napa River	Napa River	19.5	4,819
8	York Creek	Napa River	Napa River	34.2	8,451
9	Chiles Creek	Napa River	Napa River	29.5	7,293
10	Fir Canyon	Napa River	Napa River	33.2	8,195
11	Heath Canyon	Napa River	Napa River	41.0	10,139
12	Lake Hennessey	Napa River	Napa River	23.3	5,761
14	Rector Reservation	Napa River	Napa River	37.7	9,325
15	Bear Canyon	Napa River	Napa River	37.9	9,371
18	Upper Dry Creek	Napa River	Napa River	24.7	6,101
19	Milliken Reservoir	Napa River	Napa River	50.3	12,439
20	Soda Creek	Napa River	Napa River	28.6	7,070
22	Lower Dry Creek	Napa River	Napa River	23.0	5,679
24	Redwood Creek	Napa River	Napa River	28.2	6,978
29	Spencer Creek	Napa River	Napa River	36.6	9,039
30	undefined	Napa River	Napa River	38.7	9,565
34	Browns Valley	Napa River	Napa River	24.6	6,068
59	Mouth of Napa	Napa River	Napa River	145.2	35,883
13	Mouth of Napa	Napa River	n/a	174.6	43,146
16	Bear Creek	Sonoma Creek	Sonoma	21.4	5,296
17	Upper Sonoma	Sonoma Creek	Sonoma	49.1	12,140
21	Upper Calabazas	Sonoma Creek	Sonoma	46.8	11,571
23	Lower Calabazas	Sonoma Creek	Sonoma	48.9	12,073
26	Nathanson Creek	Sonoma Creek	Sonoma	37.2	9,183
27	Mouth of Sonoma	Sonoma Creek	Sonoma	122.5	30,259
38	Haraszthy Creek	Sonoma Creek	Sonoma	28.6	7,068
40	Champlin Creek	Sonoma Creek	Sonoma	19.0	4,686
43	undefined	Sonoma Creek	Sonoma	30.4	7,513
60	Mouth of Sonoma	Sonoma Creek	Sonoma	27.5	6,804
28	Lynch Creek	Petaluma River	Petaluma	42.4	10,485
31	undefined	Petaluma River	Petaluma	96.9	23,948
32	Adobe Creek	Petaluma River	Petaluma	36.5	9,016
37	undefined	Petaluma River	Petaluma	60.2	14,869
42	Upper San Antonio	Petaluma River	Petaluma	33.0	8,156
45	Stage Gulch	Petaluma River	Petaluma	30.3	7,476
46	Lower San Antonio	Petaluma River	Petaluma	60.2	14,864
47	undefined	Petaluma River	Petaluma	25.5	6,301
48	Stafford Lake	Novato	Marin Bay	126.0	31,128
51	Miller Creek	Novato	Marin Bay	30.9	7,626
53	San Anselmo Creek	San Rafael	Marin Bay	74.0	18,277

54	San Rafael Creek	San Rafael	Marin Bay	29.3	7,252
56	Old Mill Creek	San Rafael	Marin Bay	8.4	2,081
61	Gallinas Creek	Novato	Marin Bay	26.5	6,549
62	Belvedere Lagoon	San Rafael	Marin Bay	4.8	1,182
63	Belvedere Lagoon	San Rafael	Marin Bay	6.9	1,698
64	Belvedere Lagoon	San Rafael	Marin Bay	5.0	1,246
65	Belvedere Lagoon	San Rafael	Marin Bay	3.7	902
67	Old Mill Creek	San Rafael	Marin Bay	0.8	197
68	Old Mill Creek	San Rafael	Marin Bay	15.7	3,888
69	Old Mill Creek	San Rafael	Marin Bay	9.6	2,378
25	Ebabilas Creek	Estero Americano	Marin Coast	50.2	12,393
35	Upper Stemple	Estero San Antonio	Marin Coast	65.5	16,187
36	Lower Stemple	Estero San Antonio	Marin Coast	69.1	17,072
39	Keys Creek	Tomales Bay	Marin Coast	181.2	44,785
44	Nicks Cove	Tomales Bay	Marin Coast	61.9	15,302
49	Nicasio Reservoir	Tomales Bay	Marin Coast	95.7	23,638
50	Tomasini Canyon	Tomales Bay	Marin Coast	138.7	34,273
52	San Geronomo	Tomales Bay	Marin Coast	24.3	6,000
55	Pine Gulch Creek	Bolinas	Marin Coast	40.7	10,066
57	Fern Creek	Bolinas	Marin Coast	31.8	7,869
58	Rodeo Lagoon	Bolinas	Marin Coast	14.3	3,542
71	Rodeo Lagoon	Bolinas	Marin Coast	7.6	1,884
72	Audobon Canyon	Bolinas	Marin Coast	5.8	1,436
73	Pine Gulch Creek	Bolinas	Marin Coast	1.1	284
76	Laguna Lake	Tomales Bay	Marin Coast	11.1	2,747
77	Keys Creek	Tomales Bay	Marin Coast	12.4	3,055
78	Ebabilas Creek	Estero Americano	Marin Coast	23.6	5,824
73	Tomales Bay	Keys Creek	n/a	12.4	3,055
74	Estero Americano	Ebabilas Creek	n/a	23.6	5,824
75	Napa River	Upper Napa River	n/a	24.9	6,165

APPENDIX B Major Basin Assessments: tabular format

Marin Coast Major Basin

Model	Time Interval	Tmax		Tmin		PPT		Runoff		Recharge		PET		CWD	
		oC	SE	oC	SE	mm y-1	SE	mm y-1	SE	mm y-1	SE	mm y-1	SE	mm y-1	SE
Historic*	1896-20	18.3	0.1	6.5	0.1	876	258	323	43	88	7	1122	2	655	12
	1921-50	19.1	0.1	6.8	0.1	820	260	265	33	86	7	1129	4	657	14
	1951-80	19.2	0.1	6.9	0.1	911	296	346	41	96	8	1129	4	658	13
	1981-10	19.8	0.1	7.7	0.1	960	357	383	49	92	8	1160	4	684	14
GFDL A2**	2011-40	20.5	0.1	8.2	0.1	955	72	400	54	77	8	1175	2	696	15
	2041-70	21.4	0.1	9.2	0.1	907	62	387	52	72	6	1197	3	746	11
	2071-00	23.0	0.1	11.0	0.1	790	72	318	54	58	7	1236	3	818	18
GFDL B1**	2011-40	20.5	0.1	8.3	0.1	998	91	474	72	75	8	1172	2	722	12
	2041-70	21.1	0.1	8.9	0.1	952	59	396	48	78	6	1188	2	710	11
	2071-00	21.6	0.1	9.3	0.1	790	56	287	43	57	7	1197	2	748	11
PCM A2**	2011-40	20.5	0.1	7.7	0.1	974	71	401	56	79	8	1166	2	671	14
	2041-70	21.3	0.1	8.5	0.1	963	65	418	54	74	7	1186	2	713	11
	2071-00	22.4	0.1	9.6	0.1	1023	88	477	72	73	7	1210	2	737	14
PCM B1**	2011-40	20.5	0.1	7.7	0.1	1156	86	586	69	89	8	1164	2	684	15
	2041-70	20.9	0.1	8.0	0.1	1025	82	463	70	74	7	1174	2	685	14
	2071-00	21.5	0.1	8.5	0.1	999	67	446	57	72	7	1186	2	703	13

* Derived from PRISM climate data (Daly and others 2004) and Basin Characterization Model (BCM) watershed simulations for historic time steps

** Derived from referenced General Circulation Models climate projections and Basin Characterization Model (BCM) watershed simulations

Marin Bay Major Basin

Model	Time Interval	Tmax		Tmin		PPT		Runoff		Recharge		PET		CWD	
		oC	SE	oC	SE	mm y-1	SE	mm y-1	SE	mm y-1	SE	mm y-1	SE	mm y-1	SE
Historic*	1896-20	19.1	0.1	7.3	0.1	771	46	251	32	76	34	1,146	2	672	12
	1921-50	20.0	0.1	7.5	0.1	702	42	200	24	67	33	1,148	3	681	14
	1951-80	20.0	0.1	8.2	0.1	786	48	259	30	80	40	1,157	4	682	14
	1981-10	20.4	0.1	8.9	0.1	818	61	289	36	81	49	1,184	3	707	17
GFDL A2**	2011-40	21.4	0.1	9.5	0.1	856	68	313	41	80	11	1,203	10	713	17
	2041-70	22.3	0.1	10.5	0.1	803	56	301	38	72	8	1,226	14	765	12
	2071-00	24.0	0.1	12.2	0.1	687	64	242	40	58	8	1,267	16	839	18
GFDL B1**	2011-40	21.3	0.1	9.5	0.1	879	82	361	54	82	11	1,200	2	738	14
	2041-70	22.0	0.1	10.1	0.1	831	53	299	36	75	8	1,217	2	731	11
	2071-00	22.4	0.1	10.5	0.1	691	50	220	31	55	7	1,225	2	772	12
PCM A2**	2011-40	21.3	0.1	9.0	0.1	866	67	309	43	81	10	1,194	2	692	15
	2041-70	22.2	0.1	9.8	0.1	856	61	321	42	77	9	1,215	2	729	11
	2071-00	23.4	0.1	10.9	0.1	914	80	366	54	83	10	1,240	2	748	16
PCM B1**	2011-40	21.3	0.1	8.9	0.1	1,024	80	442	54	102	12	1,192	2	693	15
	2041-70	21.7	0.1	9.2	0.1	902	75	349	53	81	10	1,202	2	704	14
	2071-00	22.4	0.1	9.8	0.1	879	64	338	45	75	9	1,214	2	721	13

* Derived from PRISM climate data (Daly and others 2004) and Basin Characterization Model (BCM) watershed simulations for historic time steps

** Derived from referenced General Circulation Models climate projections and Basin Characterization Model (BCM) watershed simulations

Petaluma River Major Basin

Model	Time Interval	Tmax		Tmin		PPT		Runoff		Recharge		PET		CWD	
		oC	SE	oC	SE	mm y-1	SE	mm y-1	SE	mm y-1	SE	mm y-1	SE	mm y-1	SE
Historic*	1896-20	20.0	0.1	5.8	0.1	700	42	138	21	72	8	1155	2	663	18
	1921-50	21.0	0.1	6.1	0.1	664	39	115	15	66	7	1161	4	680	19
	1951-80	21.1	0.1	6.4	0.1	710	42	140	17	77	8	1166	4	676	19
	1981-10	21.5	0.1	7.5	0.1	745	54	162	23	80	11	1201	4	698	23
GFDL A2**	2011-40	22.5	0.1	8.1	0.1	771	58	166	23	94	14	1218	2	708	24
	2041-70	23.4	0.1	9.2	0.1	719	49	153	23	82	12	1242	3	760	17
	2071-00	25.1	0.1	11.2	0.2	619	58	126	23	66	12	1284	3	857	26
GFDL B1**	2011-40	22.5	0.1	8.1	0.2	805	73	208	34	108	99	1216	3	728	23
	2041-70	23.1	0.1	8.8	0.1	769	49	167	23	90	63	1233	2	721	18
	2071-00	23.6	0.1	9.3	0.1	649	46	124	20	64	50	1243	2	783	19
PCM A2**	2011-40	22.4	0.1	7.5	0.1	785	58	166	25	91	13	1209	2	682	22
	2041-70	23.3	0.1	8.4	0.1	779	51	174	24	91	13	1230	2	717	18
	2071-00	24.4	0.1	9.6	0.1	836	72	209	36	104	17	1256	2	734	25
PCM B1**	2011-40	22.5	0.1	0.1	0.2	805	73	208	34	108	18	1216	3	728	23
	2041-70	23.1	0.1	0.1	0.1	769	49	167	23	90	11	1233	2	721	18
	2071-00	23.6	0.1	0.1	0.1	649	46	124	20	64	9	1243	2	783	19

* Derived from PRISM climate data (Daly and others 2004) and Basin Characterization Model (BCM) watershed simulations for historic time steps
 ** Derived from referenced General Circulation Models climate projections and Basin Characterization Model (BCM) watershed simulations

Sonoma Creek Major Basin

Model	Time Interval	Tmax		Tmin		PPT		Runoff		Recharge		PET		CWD	
		oC	SE	oC	SE	mm y-1	SE	mm y-1	SE	mm y-1	SE	mm y-1	SE	mm y-1	SE
Historic	1896-20	20.7	0.1	5.7	0.1	812	48	253	31	84	7	1,173	2	697	16
	1921-50	21.4	0.1	6.0	0.1	759	44	214	23	81	6	1,173	4	713	18
	1951-80	21.7	0.1	6.6	0.1	830	48	262	26	90	8	1,186	4	710	18
	1981-10	22.0	0.1	7.7	0.1	876	62	289	33	94	10	1,220	4	727	23
GFDL A2	2011-40	23.2	0.1	8.2	0.1	883	66	269	33	118	15	1,240	13	746	22
	2041-70	24.2	0.1	9.2	0.1	840	57	262	34	107	12	1,263	15	792	17
	2071-00	25.9	0.1	11.0	0.2	706	65	207	32	85	12	1,301	17	886	24
GFDL B1	2011-40	23.1	0.1	8.4	0.1	931	86	325	49	130	18	1,240	3	764	20
	2041-70	23.8	0.1	9.1	0.1	875	57	261	32	114	12	1,255	2	756	16
	2071-00	24.3	0.1	9.5	0.1	747	53	209	29	84	10	1,265	2	810	18
PCM A2	2011-40	22.1	0.1	7.6	0.1	878	62	289	33	95	10	1,219	4	726	22
	2041-70	23.6	0.1	8.0	0.1	897	45	276	26	116	9	1,241	2	736	13
	2071-00	25.2	0.1	9.6	0.1	961	84	329	50	128	17	1,277	2	773	22
PCM B1	2011-40	23.1	0.1	7.6	0.1	1,073	78	389	44	156	18	1,229	2	701	20
	2041-70	23.6	0.1	7.9	0.1	931	79	300	47	121	16	1,238	2	728	22
	2071-00	24.3	0.1	8.5	0.1	923	65	297	39	116	12	1,252	2	742	19

* Derived from PRISM climate data (Daly and others 2004) and Basin Characterization Model (BCM) watershed simulations for historic time steps
 ** Derived from referenced General Circulation Models climate projections and Basin Characterization Model (BCM) watershed simulations

Napa River Major Basin

Model	Time Interval	Tmax		Tmin		PPT		Runoff		Recharge		PET		CWD	
		oC	SE	oC	SE	mm y-1	SE	mm y-1	SE	mm y-1	SE	mm y-1	SE	mm y-1	SE
Historic	1896-20	20.7	0.1	6.1	0.1	837	51	243	34	109	9	1178	2	691	15
	1921-50	21.5	0.2	6.4	0.1	782	46	195	25	104	9	1181	4	702	17
	1951-80	21.7	0.1	7.1	0.1	870	50	257	29	120	11	1194	4	702	16
	1981-10	22.2	0.1	7.9	0.1	913	61	282	35	123	12	1224	4	715	20
GFDL A2	2011-40	23.2	0.1	8.5	0.1	905	70	250	36	153	19	1242	3	739	20
	2041-70	24.2	0.1	9.5	0.1	868	61	249	37	142	14	1264	3	785	16
	2071-00	25.8	0.1	11.1	0.1	728	67	194	35	109	15	1300	3	873	23
GFDL B1	2011-40	23.2	0.1	8.4	0.1	967	90	323	54	164	21	1239	3	758	18
	2041-70	23.9	0.1	9.1	0.1	901	59	246	35	151	15	1254	3	749	14
	2071-00	24.3	0.1	9.5	0.1	772	56	197	32	110	13	1264	2	796	16
PCM A2	2011-40	23.2	0.1	8.0	0.1	925	72	254	40	153	18	1234	2	716	19
	2041-70	24.2	0.1	8.9	0.1	932	62	276	40	150	15	1256	2	749	14
	2071-00	25.3	0.1	10.0	0.1	994	88	331	55	160	19	1280	2	774	20
PCM B1	2011-40	23.2	0.1	8.0	0.1	1106	81	382	49	194	19	1233	2	703	18
	2041-70	23.7	0.1	8.3	0.1	955	82	292	51	150	18	1242	2	728	20
	2071-00	24.4	0.1	8.9	0.1	965	71	297	44	153	16	1257	2	740	18

* Derived from PRISM climate data (Daly and others 2004) and Basin Characterization Model (BCM) watershed simulations for historic time steps

** Derived from referenced General Circulation Models climate projections and Basin Characterization Model (BCM) watershed simulations